2008

The effects of abnormal prion protein accumulation on retinal morphology and function in sheep and cattle

Jodi D. Smith
Iowa State University

The effects of abnormal prion protein accumulation on retinal morphology and function in sheep and cattle

by

Jodi D. Smith

A dissertation submitted to the graduate faculty

in partial fulfillment of the requirements for the degree of

DOCTOR OF PHILOSOPHY

Major: Veterinary Anatomy

Program of Study Committee:
M. Heather West Greenlee, Major Professor
Justin Greenlee
Jesse Hostetter
Donald Sakaguchi
Etsuro Uemura

Iowa State University

Ames, Iowa

2008

TABLE OF CONTENTS

ABSTRACT iii

CHAPTER 1. GENERAL INTRODUCTION 1
Dissertation Organization 1
Introduction 1
Literature Review 2
References 12

CHAPTER 2. RETINAL CELL TYPES ARE DIFFERENTIALLY AFFECTED IN SHEEP WITH SCRAPIE 19
Abstract 19
Introduction 20
Materials and Methods 21
Results 23
Discussion 26
Acknowledgments 30
References 31
Figure Legends 34
Figures 36

CHAPTER 3. RETINAL FUNCTION AND MORPHOLOGY ARE ALTERED IN CATTLE EXPERIMENTALLY INFECTED WITH TRANSMISSIBLE MINK ENCEPHALOPATHY 40
Abstract 40
Introduction 40
Results 42
Discussion 43
Materials and Methods 45
Acknowledgments 47
References 47
Figure Legends 48
Figures 51

CHAPTER 4. GENERAL CONCLUSIONS 55
Summary 55
Recommendations for Future Research 56
Concluding Remarks 58
References 58

ABSTRACT

Transmissible spongiform encephalopathies (TSE) encompass a group of unique, invariably fatal neurodegenerative diseases, which affect humans and animals. Accumulation of an abnormal form of the prion protein (PrP^{Sc}) in the central nervous system serves as their pathologic underpinning. The pathogenesis of TSE remains unclear, and the specific effects of PrP^{Sc} on cells of the nervous system have yet to be completely resolved. Previous studies have identified the accumulation of PrP^{Sc} within the retina, the thin, highly organized piece of neural tissue lining the posterior aspect of the eye. The purpose of this dissertation was to investigate the effects of PrP^{Sc} accumulation on retinal cellular morphology and function.

Using morphologic and functional analyses, we have identified alterations in retinal cellular morphology and function in sheep and cattle infected with TSE. We examined the effects of PrP^{Sc} on retinal cellular morphology in sheep affected with their naturally occurring TSE, scrapie, using immunohistochemistry (IHC). We demonstrated alteration of immunoreactivity patterns of rod bipolar cell, retinal ganglion cell, and Müller glia specific markers. Immunoreactivity patterns of cholinergic amacrine cell and conventional synapse markers were similar to scrapie free control sheep. In cattle infected with a bovine-adapted isolate of transmissible mink encephalopathy (TME), we combined functional (electroretinography) and morphologic (IHC) analyses to investigate the impact of TSE infection on the bovine retina. We demonstrated altered retinal function during the preclinical phase of disease, evidenced by prolonged ERG b-wave implicit time, and during the clinical phase, evidenced by prolonged implicit time and decreased amplitude of the b-wave. Morphologic abnormalities consistent with spongiform change were demonstrated in the retina of TME-affected cattle, and immunoreactivity patterns of rod bipolar cell and Müller glia markers were altered. Our results contribute novel and important information on the response of the retina to TSE.

CHAPTER 1. GENERAL INTRODUCTION

Dissertation Organization

This dissertation includes two manuscripts relevant to this doctoral work, which have either been published in or submitted for publication in peer-reviewed journals. These manuscripts constitute the bulk of the dissertation and are preceded by statements on the research problem, significance of the research topic, and a review of the literature, followed by a general discussion of the findings and recommendations for future research.

Introduction

Transmissible spongiform encephalopathies (TSEs) are a group of invariably fatal neurodegenerative diseases affecting many mammalian species, including humans. TSEs are characterized by accumulation of abnormal prion protein (PrP^{Sc}) in the central nervous system (CNS). PrP^{Sc} also accumulates within the retinas of many TSE-affected animals and humans. Alterations in morphology and protein expression in CNS neurons have been reported in rodent models of TSEs, but there is a scarcity of information on specifically how various cell populations within the CNS are affected in non-rodent models or natural host species of TSEs (e.g. sheep with scrapie). The retina possesses many attributes, which make it a suitable model for studying potential alterations in the morphology and function of neurons and glia in TSE-infected animals. The retina is a highly organized structure with well characterized cell types, PrP^{Sc} has been shown to accumulate within the retina, and retinal function can be assessed as disease progresses. How retinal cells may be affected both morphologically and functionally in TSE-infected animals, particularly livestock species, is not known. The central hypothesis, which has guided this doctoral work, is that retinal morphology and function are altered in TSE-infected livestock species. To test this proposition, retinas from sheep affected with scrapie and cattle affected with transmissible mink encephalopathy (TME) were examined with immunohistochemistry using antibodies directed against specific retinal cell types to evaluate protein expression and cellular morphology of retinal neurons and glia. The purpose of these experiments was to establish whether neurons and glia are differentially affected in the retinas of TSE-affected sheep and cattle. Additionally, to evaluate retinal function in TME-infected cattle, flash electroretinography was used to evaluate non-inoculated, pre-clinical, and clinically affected

cattle with TME. The purpose of this set of experiments was to determine if retinal function is perturbed in TME-infected cattle. This approach of pairing morphological and functional data in order to better understand the effect(s) PrP^{Sc} may have on retinal cell subtypes, will contribute to further understanding of TSE pathobiology by providing information on the specific effects of PrP^{Sc} accumulation on cells of the nervous system.

Literature Review

Prion hypothesis

In 1997, Stanley Prusiner was awarded the Nobel Prize for his proposed prion hypothesis.[1] Prusiner coined the term 'prion' (derived from **pro**teinaceous and **in**fectious), and hypothesized that an infectious protein was responsible for causing a group of invariably fatal neurodegenerative diseases – the transmissible spongiform encephalopathies (TSEs). The prion is considered the transmissible agent of these diseases, and is composed predominantly of an abnormally folded isoform of a highly conserved cellular protein (PrP^{Sc}). The normal cellular isoform of the prion protein (PrP^{C}) is found primarily in the CNS, but has also been demonstrated in various other tissues including spleen, heart, uterus, gastrointestinal tract, skeletal muscle, and certain species-dependent blood components.[2-4] The abnormally folded, proteinase K-resistant, prion protein has been notated PrP^{Sc}, PrP^{D}, and PrP^{TSE}. It is thought that prions propagate in an autocatalytic process, whereby not only the original PrP^{Sc}, but also newly formed PrP^{Sc}, converts native PrP^{C} to the misfolded isoform.[5] PrP^{C} is necessary for propagation of PrP^{Sc}, as mice lacking PrP^{C} are refractory to scrapie infection.[6]

Physiological role of the cellular prion protein

The pathogenesis of TSEs is not well understood. One reason for this is a lack of consensus on the function of PrP^{C}. Proposed biological functions for PrP^{C} range from neuroprotection to regulation of hematopoietic stem cell renewal. One of the early functions attributed to PrP^{C} was copper binding and metabolism,[7] and subsequently, it has been demonstrated that PrP^{C} interacts with other divalent metals as well.[8] PrP^{C} also has been shown to serve a neuroprotective function. In cultures of hippocampal cell lines from mice which produce a disrupted form of the prion protein ($Prnp^{-/-}$) and wild type ($Prnp^{+/+}$) mice, removal of serum resulted in apoptosis in the $Prnp^{-/-}$ line, but not in the $Prnp^{+/+}$ line.[9] An

antioxidant function has also been ascribed to PrP^C as part of its neuroprotective role. Neuronal cell cultures derived from prion protein knockout mice were shown to be more sensitive to oxidative stress, and expressed decreased levels of superoxide dismutase relative to wild type cells.[10] Additionally, Sakudo and others[11] demonstrated that reintroduction of *Prnp* into a *Prnp*-deficient neuronal cell line resulted in upregulation of superoxide dismutase, enhanced superoxide anion clearance, and rescue from apoptosis. A potential role for PrP^C in phagocytosis has also been examined. Macrophages from *Prnp* knockout mice were demonstrated to have higher phagocytic activity relative to macrophages from wild type mice both *in vitro* and *in vivo*,[12] suggesting PrP^C may negatively regulate phagocytosis by macrophages. Recently, roles for PrP^C in the regulation of neural precursor proliferation[13] and hematopoietic stem cell renewal[14] have been proposed. By examining wild type, PrP^C overexpresser, and PrP^C knockout mice, Steele and others[13] found PrP^C positively influences neuronal precursor proliferation and differentiation. Neural precursors isolated from embryonic PrP^C overexpresser mice had an increased rate of differentiation and an increased production of mature neurons relative to precursors from wild type and PrP^C knockout mice. *In vivo* experiments in adult mice revealed PrP^C overexpressers had more proliferating cells, but there was not a significant difference in net neurogenesis between groups, indicating PrP^C is just one of many factors controlling neurogenesis. Zhang and others[14] have demonstrated PrP^C expression by murine hematopoietic stem cells. In addition, they demonstrated hematopoietic stem cells from PrP^C knockout mice had impaired self-renewal properties, which could be rescued by retrovirus-mediated reintroduction of PrP^C.

A number of recent studies have also demonstrated a synaptic localization and/or function of the prion protein.[15-19] Immunolocalization studies on the distribution of PrP^C have demonstrated a synaptic localization in rodent cerebellum[17] and in hamster and non-human primate brain.[18] PrP^C has been localized to rod photoreceptor terminals of the rat and human retina, and also amacrine cell synapses of the human retina.[20] Ultrastructural studies by Fournier and others[16] have demonstrated PrP^C immunoreactivity on synaptic structures in the hamster hippocampus with a similar distribution to that of the presynaptic protein synaptophysin. Additionally, they provided evidence for a presynaptic localization of PrP^{Sc} in the brains of scrapie-infected hamsters. Similarly, Kovacs and others[19] have reported

colocalization of PrP^{Sc} and synaptophysin in the cerebral cortices of humans with sporadic Creutzfeldt-Jakob disease. In addition to demonstrating a presynaptic location of PrP^{C} using synaptosomal fractionation techniques, Herms and others[15] also reported a correlation between synaptic activity and PrP^{C} expression in murine cerebellar slices maintained under specific biochemical conditions.

Transmissible spongiform encephalopathies (TSE)

Transmissible spongiform encephalopathies can present as inherited, sporadic, or infectious forms. All forms affect humans, and examples include familial Creutzfeldt-Jakob disease (CJD), fatal familial insomnia, Gertsmann-Sträussler-Scheinker syndrome, sporadic CJD (sCJD), kuru, and variant CJD (vCJD). To date, TSEs identified in animals have all been identified as infectious forms and include scrapie in sheep and goats, bovine spongiform encephalopathy (BSE) in cattle, transmissible mink encephalopathy (TME) in mink, and chronic wasting disease (CWD) in cervids. Transmission of the infectious forms of TSE occurs primarily via ingestion, with the exception of iatrogenic forms of CJD. Additionally, a 'species barrier' exists for TSEs, which makes cross-species transmission generally inefficient to reportedly not possible (e.g. TME to wild type mice[21]). Different strains of a particular TSE can occur, which are defined by distinct biological and biochemical features upon experimental transmission and sub-passage in rodents. Strain variation is thought to be enciphered in the many potential conformations of PrP^{Sc},[22] and strains have classically been defined in mice by their incubation period and neuropathologic lesion (vacuolation) profiles.[23, 24] Subsequently, patterns of PrP^{Sc}-immunoreactivity have been correlated with vacuolation profiles,[25, 26] and biochemical analyses have been used to generate glycoform profiles,[27] which have been applied toward prion strain typing as well.

TSE neuropathology

Accumulation of PrP^{Sc} in the central nervous system is a common and consistent pathological finding in TSEs. This accumulation is often accompanied by vacuolation (spongiform change), neuronal loss, and gliosis in the central nervous system. However, specific differences with regard to disease progression and TSE pathology can exist depending on the particular TSE, the specific strain of a given TSE, and/or the host species affected.[28-31]

Studies of the specific effects of PrP^{Sc} on cells of the CNS have largely been carried out in mice. Jeffrey and others[32] reported a significant decrease in the number of neurons in the dorsal lateral geniculate nucleus of mice intraocularly inoculated with the ME7 strain of scrapie. This loss was concomitant with the onset of vacuolation and detection of PrP^{Sc} immunolabeling. They also showed a marked decrease in synaptophysin immunolabeling in the dorsal lateral geniculate nucleus in scrapie-affected mice versus controls, which occurred after neuronal loss was established. A later study of scrapie in mice[33] reported synapse loss (quantified at the ultrastructural level) prior to neuronal loss in the hippocampus of mice intracerebrally inoculated with the ME7 strain of scrapie, indicating the synapse may be the primary target for PrP^{Sc}-induced pathology, with subsequent neuronal loss as a sequela. PrP^{Sc} immunolabeling preceded synapse loss in this study. Similarly, Cunningham and others[34] demonstrated decreased synaptophysin labeling prior to neuronal loss in the hippocampus of mice intracerebrally inoculated with ME7 scrapie. PrP^{Sc} was detected coincident with the decrease in synaptophysin labeling. Synaptic alterations have also been demonstrated concomitantly with dendritic lesions in two models of murine scrapie (ME7 and 87V scrapie strains),[35] though mice in this study were only examined at terminal stages of disease. In mice with scrapie, hippocampal neurons exhibited dendritic spine loss and occasional spherical distensions of dendrites, and synaptophysin labeling was significantly decreased, suggesting both pre- and post-synaptic elements are disrupted by scrapie infection. Jamieson and others[36] also demonstrated similar alterations in murine hippocampal dendrite morphology with the 87V scrapie strain. Examination of infected mice at sequential time points in this study, demonstrated these morphologic changes preceded PrP^{Sc} detection. In addition, terminal deoxynucleotidyl transferase-mediated uridine triphosphate nick end labeling (TUNEL) indicated apoptotic cell death shortly after the onset of altered dendritic morphology, but before PrP^{Sc} detection. Apoptosis as a mechanism for TSE-related cell death in the CNS has been proposed by a number of studies in murine models.[37-40] However, a recent study has demonstrated that overexpression of B-cell lymphoma protein 2 (Bcl-2) or lack of expression of Bcl-2-associated X protein (Bax) in mice was not protective against prion disease, suggesting that this particular apoptotic pathway is not a major contributing factor in TSE pathology.[41]

Scrapie

Scrapie, the most extensively studied of the TSEs, has been recognized as a disease of sheep for centuries in Europe and was first identified in sheep in the United States in 1947. In 1998, a new type of scrapie was identified in sheep in Norway and designated Nor98.[42] Nor98 differs from classical scrapie in the distribution of PrP^{Sc} within the brain, its Western blot profile, the absence of detectable PrP^{Sc} in the lymphoreticular system of affected sheep, and the susceptibility of sheep generally considered resistant to classical scrapie.[43] Relative susceptibility or resistance of sheep to scrapie has been attributed to three PrP^{C} gene (*Prnp*) polymorphisms.[44, 45] These are valine (V) or alanine (A) at codon 136, arginine (R) or histidine (H) at codon 154, and glutamine (Q), arginine (R), or histidine (H) at codon 171. The $A_{136}R_{154}R_{171}$ allele is associated with relative resistance to scrapie, while the $V_{136}R_{154}Q_{171}$ allele is associated with susceptibility. Absolute resistance to scrapie is not conferred by the $A_{136}R_{154}R_{171}$/ $A_{136}R_{154}R_{171}$ genotype, however, as both classical and atypical forms of scrapie have been identified in sheep of this genotype.[46, 47]

Scrapie was successfully transmitted to mice in 1961,[48] making animal studies of the disease more convenient, and leading to the identification of various strains of scrapie. Although rodents are not natural hosts of the disease, much of what is known about the specific effects of PrP^{Sc} on CNS neurons (e.g. synaptic loss, dendritic alterations) has been gathered from studies on rodent models of scrapie.[33-36] Scrapie has also been experimentally transmitted to number of other species including cattle (by the intracerebral route),[49] elk,[50] and raccoons.[51]

Transmissible mink encephalopathy (TME)

Transmissible mink encephalopathy (TME) is a TSE that has been sporadically identified in ranch-raised mink in North America. The origin of TME is unclear, but infection with a ruminant TSE, specifically of ovine or bovine origin, has been proposed as the cause.[52, 53] Bovine spongiform encephalopathy (BSE) has been successfully transmitted to mink via the intracerebral and oral routes, but resulted in different clinical and pathologic features than had been observed in mink naturally infected with TME.[54] Transmissible mink encephalopathy has been experimentally transmitted to cattle by the intracerebral route.[55, 56] Although samples were not analyzed in parallel, Hamir and others[56] reported that TME in

cattle had clinical, pathologic, and biochemical findings similar to those of BSE. Recently, clinical, biochemical, and histologic similarities have been demonstrated between TME and L-type BSE (one of three phenotypes of BSE based on molecular features of PrP^{Sc57}) in an ovine transgenic mouse line, suggesting L-type BSE is a more likely candidate for the originator of TME than are the other currently recognized types of BSE – classical and H-type BSE.[58] In addition to cattle, TME has been experimentally transmitted to sheep and goats,[59] skunks and ferrets,[60] hamsters,[61] non-human primates,[62] and raccoons[63] via the intracerebral route.

Studies on TME have provided information on TSE strain variation[64, 65] and PrP^{Sc} transmission and neuroinvasion.[66-68] Experimental infection of hamsters with TME identified two strains of TME, termed hyper and drowsy.[65] Subsequent biochemical studies of PrP^{Sc} from each strain revealed strain-specific degradation rates, distinct proteinase K cleavage sites, and a differential distribution of each strain within the brain of hamsters, suggesting the conformation of PrP^{Sc} may determine the molecular basis of TSE strain variation.[64] Experimental infection of hamsters with TME has also provided information on mechanisms of PrP^{Sc} transport within the spinal cord,[66] lymphoreticular system-independent neuroinvasion,[67] and evidence for the nasal cavity as a portal of entry for TSE infection.[68]

Current status of TSE diagnostics

Currently, definitive diagnosis of TSE in animals is based on postmortem tests including histopathologic examination of brain tissue, immunohistochemistry with anti-PrP^{C} antibodies, and Western blot analysis. Successful experimental infection of laboratory animals is an additional method of diagnosing TSE. Recently, 'rapid tests' have emerged based on the immunological detection of PrP^{Sc}.[69, 70] These tests are performed on brain tissues and consequently are only useful as postmortem diagnostic tools, and currently, all results are confirmed in national reference laboratories. To date, there are no diagnostic tools available for preclinical diagnosis of TSE. However, an experimental assay termed protein misfolding cyclic amplification (PMCA) has recently been developed, which is used to detect PrP^{Sc} by utilizing a small quantity of PrP^{Sc} to convert large amounts of PrP^{C} to PrP^{Sc} in a cyclic manner.[71] Antemortem detection of PrP^{Sc} has been demonstrated in the blood of

hamsters affected with scrapie by PMCA.[72] Subsequently, PMCA was used to detect PrP^{Sc} in the blood of hamsters infected with scrapie during the preclinical phases of disease.[73]

Retinal histology and functional organization

The retina is a thin, highly organized piece of neuroepithelial tissue that lines the posterior aspect of the globe and is responsible for the conversion of light into neural signals. The mature retina consists of two major divisions: an inner multicellular neural retina and an outer single-cell layer of neuroepithelium termed the retinal pigment epithelium. The neural retina has a characteristic laminar structure consisting of alternating cellular and synaptic (plexiform) layers. Moving sclerad (toward the sclera) to vitread (toward the vitreous chamber), the outermost layer of the neural retina consists of photoreceptor outer segments, connecting cilia, and inner segments, and is collectively referred to as the outer segment (OS) layer. Cell bodies of rod and cone photoreceptors comprise the outer nuclear layer (ONL). Located vitread to the ONL is a thin synaptic layer, the outer plexiform layer (OPL). The OPL consists of processes of bipolar cells, horizontal cells, and photoreceptors, and contains photoreceptor ribbon synapses and the non-vesicular synapses of horizontal cells. The inner nuclear layer (INL) is a heterogeneous cellular layer, which contains cell bodies of bipolar, amacrine, and horizontal cells, and Müller glia. Synaptic connections between bipolar, amacrine, and retinal ganglion cells occur in the relatively thick (compared to the OPL) inner plexiform layer (IPL). The cellular layer lying along the vitreal aspect of the IPL is the retinal ganglion cell layer (GCL), and finally, the most vitreal or inner layer of the retina is the optic fiber layer (OFL). The OFL consists of unmyelinated ganglion cell axons, which course along the vitreal surface of the retina and give rise to the optic nerve as they exit the eye at the optic disk.

Neural signals generated by photoreceptor cells are transmitted to bipolar cells, which express different types of receptors for glutamate that allow each bipolar cell type to respond to photoreceptor input in a specific way.[74] Bipolar cells express either ionotropic glutamate receptors (excitatory) or metabotropic glutamate receptors (inhibitory), which allow for a set of parallel visual pathways for shadow and highlight detection (known as OFF and ON pathways, respectively). For cone photoreceptors, this pathway is direct to OFF and ON retinal ganglion cells. Rod photoreceptors, however, communicate with only one type of

bipolar cell, an ON type, which relays signals to ganglion cells via AII and GABAergic A17 amacrine cells. These pathways relay contrast information, but require additional input at the retinal level for more precise visual discrimination. Horizontal and amacrine cells play a modulatory role in these pathways by modifying the receptive fields of bipolar cells and ganglion cells. Their activity effectively places an edge around the receptive field (i.e. places a boundary around the image), allowing for fine visual discrimination.

The major cell types of the retina have been extensively characterized, and many can be identified by predictable and distinct immunolabeling patterns. In the mammalian retina, antibodies directed against the alpha isoform of protein kinase C (PKCα) can be used as a marker of rod bipolar cells.[75, 76] Rod bipolar cells function as interneurons within the retina, relaying visual signals from rod photoreceptor cells to ganglion cells (via AII amacrine cells). PKCα-immunoreactive rod bipolar cell bodies reside at the outer margin of the INL and project axons to the vitreal border of the IPL. Immunoreactivity for vesicular glutamate transporter 1 (VGLUT1) has been demonstrated in glutamatergic terminals of photoreceptors in the OPL and terminals of bipolar cells in the IPL.[77] Amacrine cells function in modulating signaling between bipolar cells and ganglion cells in the retina. In the retina, antibodies against syntaxin 1 and choline acetyltransferase (ChAT) can be used to label amacrine cells. Amacrine cell bodies are located primarily in the INL, but 'displaced' amacrine cells are also present in the GCL. Syntaxin 1 is a synapse-associated protein involved in neurotransmitter release.[78] Syntaxin 1-immunoreactivity (-IR) is present in the OPL where it is localized to horizontal cell processes,[79] and in conventional synapses of amacrine cells in the IPL.[80] Antibodies directed against ChAT label a specific type of amacrine cell, the cholinergic amacrine cell.[76, 81, 82] ChAT-positive amacrine cells are located in the vitreal half of the INL and in the GCL, and their processes form two distinct strata in the IPL. In the retina, antibodies against microtubule-associated protein 2 (MAP2) label a subpopulation of retinal ganglion cells and their processes in the IPL, some amacrine cells, and horizontal cells.[83, 84] Glutamine synthetase (GS) is a glial enzyme involved in controlling extracellular glutamate concentrations by converting excess glutamate to glutamine. In the retina, GS is expressed by Müller glia, the primary glial cell of the retina.[76, 85] Cell bodies of Müller glia are located in the mid-INL, and their processes project sclerad to the junction between photoreceptor cell

bodies and outer segments, forming the outer limiting membrane, and vitreally to the optic fiber layer, forming the inner limiting membrane.

Retinal pathology associated with TSE

Accumulation of PrP^{Sc} has been demonstrated in the retinas of a number of natural and non-natural host species of TSEs,[50, 86-94] including humans with sporadic or variant CJD.[88, 89] Spongiform change in the inner and outer plexiform layers and retinal ganglion cell layer has been reported in one study of humans with CJD.[95] Electron microscopic examination of these retinas demonstrated vacuolization of Müller glia and disrupted photoreceptor synapses. Retinal accumulation of PrP^{Sc} has also been reported in sheep naturally[93] and experimentally[94] infected with scrapie. Histologic lesions including loss of outer limitant layer definition, OPL atrophy, and disorganization and loss of nuclei in the inner and outer nuclear layers were reported in sheep with natural scrapie,[93] but histologic retinal lesions were not observed in experimentally infected sheep.[94] In contrast to reports in natural hosts (e.g. humans with CJD, sheep with scrapie), a number of studies using TSE-infected rodents have demonstrated progressive and severe retinal degeneration.[86, 96-98] In mice, immunohistochemical labeling for PrP^{Sc} and the degree of retinal pathology varied depending on the strain of scrapie and background genetics of the mouse.[86] Although retinal PrP^{Sc} accumulation has been well documented in natural hosts infected with TSEs, there is limited information describing the effects of PrP^{Sc} accumulation on specific retinal cell types. Increased glial fibrillary acidic protein (GFAP) expression has been reported in the retinas of sheep with scrapie,[93, 94] and recent examination of retinas from sheep experimentally infected with scrapie demonstrated altered immunoreactivity patterns of rod bipolar, Müller glia, and retinal ganglion cell markers.[99]

Electroretinography

Electroretinography is a noninvasive *in vivo* assay of retinal function, which can be manipulated to provide a variety of information on the function of retinal cell subpopulations. The electroretinogram (ERG) represents a summed response of all of the cells of the retina, most often measured at the cornea, to a flash of light. It illustrates the sum of positive and negative component potentials that originate from different stages of retinal processing and overlap in time.[100] These potentials are a product of localized conductance changes in the

cell membranes of active cells, which generate inward and outward currents that also flow in the extracellular space.[101] With enough cells synchronously activated and generating light-evoked currents, extracellular potential changes can be measured at a distance (e.g. the cornea).

In its most typical form, the ERG consists of a small, initial, negative deflection, termed the a-wave, followed by a large positive deflection, the b-wave. The a-wave is primarily associated with photoreceptor activity, but pharmacological dissection studies have also identified contributions from the OFF circuitry of the retina.[101] The current consensus on the cellular origin of the b-wave is that it primarily reflects ON bipolar cell currents, with a small contribution from Müller glia as well.[101] Superimposed on the b-wave, and often not observed unless bandwidth settings are adjusted to specifically detect them, are 4-10, high frequency, low amplitude wavelets called oscillatory potentials (OPs). Most work indicates these responses are generated in the inner plexiform layer.[101]

Various factors such as light-adaptation state of the retina, and intensity, frequency, or color of the light stimulus can affect the extent to which certain cell populations contribute to the ERG. For example, scotopic ERG recordings (performed under dark conditions) predominantly assess rod photoreceptors and their pathway, while photopic recordings (performed under light conditions) primarily assess cone photoreceptor responses. Typically, ERG analysis includes measurements of the magnitude (amplitude, reported in microvolts) and time to peak (implicit time, reported in milliseconds) of both the a- and b-waves. The amplitude of the a-wave is measured from baseline to the peak of the initial negative deflection, and implicit time is reported as the time between stimulus onset and peak of the a-wave. The amplitude of the b-wave is measured from the peak of the a-wave to the peak of the following positive deflection, and implicit time is reported as the time between stimulus onset and peak of the b-wave.

Functional consequences of TSE on the retina

Evidence of TSE-related neuro-ophthalmologic impairment has been reported in humans and mice. Approximately one-half of CJD patients exhibit visual symptoms at some point during the course of disease.[102] Alterations in retinal function, specifically diminished b-wave amplitude, have been documented in CJD patients using electroretinography.[95, 103]

Mice clinically affected with scrapie also have an abnormal ERG characterized by a progressive reduction of b-wave amplitude.[104] To date, the use of electroretinography in the evaluation of TSE-infected livestock species has not been reported. However, electroretinography has been used successfully in the evaluation of retinal function in normal Suffolk sheep[105] and normal Holstein cattle.[106] Evaluation of the ERG in various breeds of dairy calves revealed the presence of all aspects of the adult ERG in recordings obtained by 24 hours after birth.[107] ERG a- and b-wave amplitude and implicit time values were within the range for adults from birth and by 2 weeks of age, respectively. Strain and others also found the ERG to be normal in ruminants affected with listeriosis and thiamine-responsive polioencephalomalacia.[108]

References

1. Prusiner, S. B. Prions. Proc Natl Acad Sci U S A 95, 13363-83 (1998).
2. Horiuchi, M., Yamazaki, N., Ikeda, T., Ishiguro, N. & Shinagawa, M. A cellular form of prion protein (PrP^C) exists in many non-neuronal tissues of sheep. J Gen Virol 76 (Pt 10), 2583-7 (1995).
3. Li, R. et al. The expression and potential function of cellular prion protein in human lymphocytes. Cell Immunol 207, 49-58 (2001).
4. Barclay, G. R., Houston, E. F., Halliday, S. I., Farquhar, C. F. & Turner, M. L. Comparative analysis of normal prion protein expression on human, rodent, and ruminant blood cells by using a panel of prion antibodies. Transfusion 42, 517-26 (2002).
5. Bieschke, J. et al. Autocatalytic self-propagation of misfolded prion protein. Proc Natl Acad Sci U S A 101, 12207-11 (2004).
6. Prusiner, S. B. et al. Ablation of the prion protein (PrP) gene in mice prevents scrapie and facilitates production of anti-PrP antibodies. Proc Natl Acad Sci U S A 90, 10608-12 (1993).
7. Brown, D. R. et al. The cellular prion protein binds copper in vivo. Nature 390, 684-7 (1997).
8. Choi, C. J., Kanthasamy, A., Anantharam, V. & Kanthasamy, A. G. Interaction of metals with prion protein: possible role of divalent cations in the pathogenesis of prion diseases. Neurotoxicology 27, 777-87 (2006).
9. Kuwahara, C. et al. Prions prevent neuronal cell-line death. Nature 400, 225-6 (1999).
10. Brown, D. R., Nicholas, R. S. & Canevari, L. Lack of prion protein expression results in a neuronal phenotype sensitive to stress. J Neurosci Res 67, 211-24 (2002).
11. Sakudo, A. et al. Impairment of superoxide dismutase activation by N-terminally truncated prion protein (PrP) in PrP-deficient neuronal cell line. Biochem Biophys Res Commun 308, 660-7 (2003).
12. de Almeida, C. J. et al. The cellular prion protein modulates phagocytosis and inflammatory response. J Leukoc Biol 77, 238-46 (2005).

13. Steele, A. D., Emsley, J. G., Ozdinler, P. H., Lindquist, S. & Macklis, J. D. Prion protein (PrP^c) positively regulates neural precursor proliferation during developmental and adult mammalian neurogenesis. Proc Natl Acad Sci U S A 103, 3416-21 (2006).
14. Zhang, C. C., Steele, A. D., Lindquist, S. & Lodish, H. F. Prion protein is expressed on long-term repopulating hematopoietic stem cells and is important for their self-renewal. Proc Natl Acad Sci U S A 103, 2184-9 (2006).
15. Herms, J. et al. Evidence of presynaptic location and function of the prion protein. J Neurosci 19, 8866-75 (1999).
16. Fournier, J. G., Escaig-Haye, F. & Grigoriev, V. Ultrastructural localization of prion proteins: physiological and pathological implications. Microsc Res Tech 50, 76-88 (2000).
17. Haeberle, A. M. et al. Synaptic prion protein immuno-reactivity in the rodent cerebellum. Microsc Res Tech 50, 66-75 (2000).
18. Moya, K. L. et al. Immunolocalization of the cellular prion protein in normal brain. Microsc Res Tech 50, 58-65 (2000).
19. Kovacs, G. G., Preusser, M., Strohschneider, M. & Budka, H. Subcellular localization of disease-associated prion protein in the human brain. Am J Pathol 166, 287-94 (2005).
20. Gong, J. et al. The toxicity of the PrP106-126 prion peptide on cultured photoreceptors correlates with the prion protein distribution in the mammalian and human retina. Am J Pathol 170, 1314-24 (2007).
21. Taylor, D. M., Dickinson, A. G., Fraser, H. & Marsh, R. F. Evidence that transmissible mink encephalopathy agent is biologically inactive in mice. Neuropathol Appl Neurobiol 12, 207-15 (1986).
22. Telling, G. C. et al. Evidence for the conformation of the pathologic isoform of the prion protein enciphering and propagating prion diversity. Science 274, 2079-82 (1996).
23. Fraser, H. & Dickinson, A. G. The sequential development of the brain lesion of scrapie in three strains of mice. J Comp Pathol 78, 301-11 (1968).
24. Fraser, H. & Dickinson, A. G. Scrapie in mice. Agent-strain differences in the distribution and intensity of grey matter vacuolation. J Comp Pathol 83, 29-40 (1973).
25. Bruce, M. E., McBride, P. A. & Farquhar, C. F. Precise targeting of the pathology of the sialoglycoprotein, PrP, and vacuolar degeneration in mouse scrapie. Neurosci Lett 102, 1-6 (1989).
26. DeArmond, S. J. et al. Three scrapie prion isolates exhibit different accumulation patterns of the prion protein scrapie isoform. Proc Natl Acad Sci U S A 90, 6449-53 (1993).
27. Somerville, R. A. et al. Biochemical typing of scrapie strains. Nature 386, 564 (1997).
28. Bruce, M. E., McConnell, I., Fraser, H. & Dickinson, A. G. The disease characteristics of different strains of scrapie in Sinc congenic mouse lines: implications for the nature of the agent and host control of pathogenesis. J Gen Virol 72 (Pt 3), 595-603 (1991).
29. Bruce, M. E. et al. Strain characterization of natural sheep scrapie and comparison with BSE. J Gen Virol 83, 695-704 (2002).

30. Fraser, H. Diversity in the neuropathology of scrapie-like diseases in animals. Br Med Bull 49, 792-809 (1993).
31. Jeffrey, M. et al. Differential diagnosis of infections with the bovine spongiform encephalopathy (BSE) and scrapie agents in sheep. J Comp Pathol 125, 271-84 (2001).
32. Jeffrey, M. et al. Early unsuspected neuron and axon terminal loss in scrapie-infected mice revealed by morphometry and immunocytochemistry. Neuropathol Appl Neurobiol 21, 41-9 (1995).
33. Jeffrey, M. et al. Synapse loss associated with abnormal PrP precedes neuronal degeneration in the scrapie-infected murine hippocampus. Neuropathol Appl Neurobiol 26, 41-54 (2000).
34. Cunningham, C. et al. Synaptic changes characterize early behavioural signs in the ME7 model of murine prion disease. Eur J Neurosci 17, 2147-55 (2003).
35. Belichenko, P. V., Brown, D., Jeffrey, M. & Fraser, J. R. Dendritic and synaptic alterations of hippocampal pyramidal neurones in scrapie-infected mice. Neuropathol Appl Neurobiol 26, 143-9 (2000).
36. Jamieson, E., Jeffrey, M., Ironside, J. W. & Fraser, J. R. Apoptosis and dendritic dysfunction precede prion protein accumulation in 87V scrapie. Neuroreport 12, 2147-53 (2001).
37. Jamieson, E., Jeffrey, M., Ironside, J. W. & Fraser, J. R. Activation of Fas and caspase 3 precedes PrP accumulation in 87V scrapie. Neuroreport 12, 3567-72 (2001).
38. Giese, A., Groschup, M. H., Hess, B. & Kretzschmar, H. A. Neuronal cell death in scrapie-infected mice is due to apoptosis. Brain Pathol 5, 213-21 (1995).
39. Chiesa, R. et al. Accumulation of protease-resistant prion protein (PrP) and apoptosis of cerebellar granule cells in transgenic mice expressing a PrP insertional mutation. Proc Natl Acad Sci U S A 97, 5574-9 (2000).
40. Chiesa, R. et al. Bax deletion prevents neuronal loss but not neurological symptoms in a transgenic model of inherited prion disease. Proc Natl Acad Sci U S A 102, 238-43 (2005).
41. Steele, A. D. et al. Diminishing apoptosis by deletion of Bax or overexpression of Bcl-2 does not protect against infectious prion toxicity in vivo. J Neurosci 27, 13022-7 (2007).
42. Benestad, S. L. et al. Cases of scrapie with unusual features in Norway and designation of a new type, Nor98. Vet Rec 153, 202-8 (2003).
43. Benestad, S. L., Arsac, J. N., Goldmann, W. & Noremark, M. Atypical/Nor98 scrapie: properties of the agent, genetics, and epidemiology. Vet Res 39, 19 (2008).
44. Clouscard, C. et al. Different allelic effects of the codons 136 and 171 of the prion protein gene in sheep with natural scrapie. J Gen Virol 76 (Pt 8), 2097-101 (1995).
45. Baylis, M. et al. Scrapie epidemic in a fully PrP-genotyped sheep flock. J Gen Virol 83, 2907-14 (2002).
46. Le Dur, A. et al. A newly identified type of scrapie agent can naturally infect sheep with resistant PrP genotypes. Proc Natl Acad Sci U S A 102, 16031-6 (2005).
47. Groschup, M. H. et al. Classic scrapie in sheep with the ARR/ARR prion genotype in Germany and France. Emerg Infect Dis 13, 1201-7 (2007).

48. Chandler, R. Encephalopathy in mice produced by inoculation with scrapie brain material. Lancet, 1378-1379 (1961).
49. Cutlip, R. C. et al. Intracerebral transmission of scrapie to cattle. J Infect Dis 169, 814-20 (1994).
50. Hamir, A. N. et al. Transmission of sheep scrapie to elk (*Cervus elaphus nelsoni*) by intracerebral inoculation: final outcome of the experiment. J Vet Diagn Invest 16, 316-21 (2004).
51. Hamir, A. N. et al. Experimental inoculation of scrapie and chronic wasting disease agents in raccoons (*Procyon lotor*). Vet Rec 153, 121-3 (2003).
52. Hanson, R. P. et al. Susceptibility of mink to sheep scrapie. Science 172, 859-61 (1971).
53. Marsh, R. F., Bessen, R. A., Lehmann, S. & Hartsough, G. R. Epidemiological and experimental studies on a new incident of transmissible mink encephalopathy. J Gen Virol 72 (Pt 3), 589-94 (1991).
54. Robinson, M. M. et al. Experimental infection of mink with bovine spongiform encephalopathy. J Gen Virol 75 (Pt 9), 2151-5 (1994).
55. Robinson, M. M. et al. Experimental infection of cattle with the agents of transmissible mink encephalopathy and scrapie. J Comp Pathol 113, 241-51 (1995).
56. Hamir, A. N., Kunkle, R. A., Miller, J. M., Bartz, J. C. & Richt, J. A. First and second cattle passage of transmissible mink encephalopathy by intracerebral inoculation. Vet Pathol 43, 118-26 (2006).
57. Jacobs, J. G. et al. Molecular discrimination of atypical bovine spongiform encephalopathy strains from a geographical region spanning a wide area in Europe. J Clin Microbiol 45, 1821-9 (2007).
58. Baron, T., Bencsik, A., Biacabe, A. G., Morignat, E. & Bessen, R. A. Phenotypic similarity of transmissible mink encephalopathy in cattle and L-type bovine spongiform encephalopathy in a mouse model. Emerg Infect Dis 13, 1887-94 (2007).
59. Hadlow, W. J., Race, R. E. & Kennedy, R. C. Experimental infection of sheep and goats with transmissible mink encephalopathy virus. Can J Vet Res 51, 135-44 (1987).
60. Eckroade, R. J., ZuRhein, G. M. & Hanson, R. P. Transmissible mink encephalopathy in carnivores: clinical, light and electron microscopic studies in raccons, skunks and ferrets. J Wildl Dis 9, 229-40 (1973).
61. Marsh, R. F. & Kimberlin, R. H. Comparison of scrapie and transmissible mink encephalopathy in hamsters. II. Clinical signs, pathology, and pathogenesis. J Infect Dis 131, 104-10 (1975).
62. Eckroade, R. J., Zu Rhein, G. M., Marsh, R. F. & Hanson, R. P. Transmissible mink encephalopathy: experimental transmission to the squirrel monkey. Science 169, 1088-90 (1970).
63. Hamir, A. N. et al. Transmission of transmissible mink encephalopathy to raccoons (*Procyon lotor*) by intracerebral inoculation. J Vet Diagn Invest 16, 57-63 (2004).
64. Bessen, R. A. & Marsh, R. F. Distinct PrP properties suggest the molecular basis of strain variation in transmissible mink encephalopathy. J Virol 68, 7859-68 (1994).

65. Bessen, R. A. & Marsh, R. F. Identification of two biologically distinct strains of transmissible mink encephalopathy in hamsters. J Gen Virol 73 (Pt 2), 329-34 (1992).
66. Bartz, J. C., Kincaid, A. E. & Bessen, R. A. Retrograde transport of transmissible mink encephalopathy within descending motor tracts. J Virol 76, 5759-68 (2002).
67. Bartz, J. C., Dejoia, C., Tucker, T., Kincaid, A. E. & Bessen, R. A. Extraneural prion neuroinvasion without lymphoreticular system infection. J Virol 79, 11858-63 (2005).
68. Kincaid, A. E. & Bartz, J. C. The nasal cavity is a route for prion infection in hamsters. J Virol 81, 4482-91 (2007).
69. Schaller, O. et al. Validation of a western immunoblotting procedure for bovine PrP(Sc) detection and its use as a rapid surveillance method for the diagnosis of bovine spongiform encephalopathy (BSE). Acta Neuropathol 98, 437-43 (1999).
70. Moynagh, J. & Schimmel, H. Tests for BSE evaluated. Bovine spongiform encephalopathy. Nature 400, 105 (1999).
71. Saborio, G. P., Permanne, B. & Soto, C. Sensitive detection of pathological prion protein by cyclic amplification of protein misfolding. Nature 411, 810-3 (2001).
72. Castilla, J., Saa, P. & Soto, C. Detection of prions in blood. Nat Med 11, 982-5 (2005).
73. Saa, P., Castilla, J. & Soto, C. Presymptomatic detection of prions in blood. Science 313, 92-4 (2006).
74. Kolb, H. Functional organization of the retina. In Heckenlively JR and Arden GB (eds): Priniciples and practice of clinical electrophysiology of vision, 2nd Ed. Cambride, MA, MIT Press. (ed. Heckenlively JR, A. G.) (MIT Press, Cambridge, MA, 2006).
75. Greferath, U., Grunert, U. & Wassle, H. Rod bipolar cells in the mammalian retina show protein kinase C-like immunoreactivity. J Comp Neurol 301, 433-42 (1990).
76. Haverkamp, S. & Wassle, H. Immunocytochemical analysis of the mouse retina. J Comp Neurol 424, 1-23 (2000).
77. Johnson, J. et al. Vesicular neurotransmitter transporter expression in developing postnatal rodent retina: GABA and glycine precede glutamate. J Neurosci 23, 518-29 (2003).
78. Rothman, J. E. Mechanisms of intracellular protein transport. Nature 372, 55-63 (1994).
79. Hirano, A. A., Brandstatter, J. H. & Brecha, N. C. Cellular distribution and subcellular localization of molecular components of vesicular transmitter release in horizontal cells of rabbit retina. J Comp Neurol 488, 70-81 (2005).
80. Morgans, C. W., Brandstatter, J. H., Kellerman, J., Betz, H. & Wassle, H. A SNARE complex containing syntaxin 3 is present in ribbon synapses of the retina. J Neurosci 16, 6713-21 (1996).
81. Rodieck, R. W. & Marshak, D. W. Spatial density and distribution of choline acetyltransferase immunoreactive cells in human, macaque, and baboon retinas. J Comp Neurol 321, 46-64 (1992).
82. Voigt, T. Cholinergic amacrine cells in the rat retina. J Comp Neurol 248, 19-35 (1986).

83. Okabe, S., Shiomura, Y. & Hirokawa, N. Immunocytochemical localization of microtubule-associated proteins 1A and 2 in the rat retina. Brain Res 483, 335-46 (1989).
84. Tucker, R. P. & Matus, A. I. Microtubule-associated proteins characteristic of embryonic brain are found in the adult mammalian retina. Dev Biol 130, 423-34 (1988).
85. Riepe, R. E. & Norenburg, M. D. Muller cell localisation of glutamine synthetase in rat retina. Nature 268, 654-5 (1977).
86. Foster, J., Farquhar, C., Fraser, J. & Somerville, R. Immunolocalization of the prion protein in scrapie affected rodent retinas. Neurosci Lett 260, 1-4 (1999).
87. Spraker, T. R. et al. Comparison of histological lesions and immunohistochemical staining of proteinase-resistant prion protein in a naturally occurring spongiform encephalopathy of free-ranging mule deer (*Odocoileus hemionus*) with those of chronic wasting disease of captive mule deer. Vet Pathol 39, 110-9 (2002).
88. Head, M. W. et al. Prion protein accumulation in eyes of patients with sporadic and variant Creutzfeldt-Jakob disease. Invest Ophthalmol Vis Sci 44, 342-6 (2003).
89. Head, M. W. et al. Abnormal prion protein in the retina of the most commonly occurring subtype of sporadic Creutzfeldt-Jakob disease. Br J Ophthalmol 89, 1131-3 (2005).
90. Valdez, R. A., Rock, M. J., Anderson, A. K. & O'Rourke, K. I. Immunohistochemical detection and distribution of prion protein in a goat with natural scrapie. J Vet Diagn Invest 15, 157-62 (2003).
91. Hamir, A. N. et al. Experimental transmission of sheep scrapie by intracerebral and oral routes to genetically susceptible Suffolk sheep in the United States. J Vet Diagn Invest 17, 3-9 (2005).
92. Kercher, L., Favara, C., Chan, C. C., Race, R. & Chesebro, B. Differences in scrapie-induced pathology of the retina and brain in transgenic mice that express hamster prion protein in neurons, astrocytes, or multiple cell types. Am J Pathol 165, 2055-67 (2004).
93. Hortells, P. et al. Pathological findings in retina and visual pathways associated to natural Scrapie in sheep. Brain Res 1108, 188-94 (2006).
94. Greenlee, J. J., Hamir, A. N. & West Greenlee, M. H. Abnormal prion accumulation associated with retinal pathology in experimentally inoculated scrapie-affected sheep. Vet Pathol 43, 733-9 (2006).
95. de Seze, J. et al. Creutzfeldt-Jakob disease: neurophysiologic visual impairments. Neurology 51, 962-7 (1998).
96. Hogan, R. N., Kingsbury, D. T., Baringer, J. R. & Prusiner, S. B. Retinal degeneration in experimental Creutzfeldt-Jakob disease. Lab Invest 49, 708-15 (1983).
97. Buyukmihci, N., Goehring-Harmon, F. & Marsh, R. F. Photoreceptor degeneration preceding clinical scrapie encephalopathy in hamsters. J Comp Neurol 205, 49-54 (1982).
98. Hogan, R. N., Baringer, J. R. & Prusiner, S. B. Progressive retinal degeneration in scrapie-infected hamsters: a light and electron microscopic analysis. Lab Invest 44, 34-42 (1981).

99. Smith, J. D., Greenlee, J. J., Hamir, A. N. & West Greenlee, M. H. Retinal cell types are differentially affected in sheep with scrapie. J Comp Pathol 138, 12-22 (2008).
100. Granit, R. The components of the retinal action potential in mammals and their relation to the discharge in the optic nerve. J Physiol 77, 207-39 (1933).
101. Frishman, L. Origins of the electroretinogram. In Heckenlively JR and Arden GB (eds): Priniciples and practice of clinical electrophysiology of vision, 2nd Ed. Cambride, MA, MIT Press. (ed. Heckenlively JR, A. G.) (MIT Press, Cambridge, MA, 2006).
102. Armstrong, R. A. Creutzfeldt-Jakob disease and vision. Clin Exp Optom 89, 3-9 (2006).
103. Katz, B. J., Warner, J. E., Digre, K. B. & Creel, D. J. Selective loss of the electroretinogram B-wave in a patient with Creutzfeldt-Jakob disease. J Neuroophthalmol 20, 116-8 (2000).
104. Curtis, R., Fraser, H., Foster, J. D. & Scott, J. R. The correlation of electroretinographic and histopathological findings in the eyes of mice infected with the 79A strain of scrapie. Neuropathol Appl Neurobiol 15, 75-89 (1989).
105. Strain, G. M., Claxton, M. S., Prescott-Mathews, J. S. & LaPhand, D. J. Electroretinogram and visual-evoked potential measurements in sheep. Can J Vet Res 55, 1-4 (1991).
106. Strain, G. M., Olcott, B. M. & Hokett, L. D. Electroretinogram and visual-evoked potential measurements in Holstein cows. Am J Vet Res 47, 1079-81 (1986).
107. Strain, G. M., Graham, M. C., Claxton, M. S. & Olcott, B. M. Postnatal development of brainstem auditory-evoked potentials, electroretinograms, and visual-evoked potentials in the calf. J Vet Intern Med 3, 231-7 (1989).
108. Strain, G. M., Claxton, M. S., Olcott, B. M. & Turnquist, S. E. Visual-evoked potentials and electroretinograms in ruminants with thiamine-responsive polioencephalomalacia or suspected listeriosis. Am J Vet Res 51, 1513-7 (1990).

CHAPTER 2. RETINAL CELL TYPES ARE DIFFERENTIALLY AFFECTED IN SHEEP WITH SCRAPIE[1]

A paper published in the
Journal of Comparative Pathology, 2008, 138:12-22

Jodi D. Smith[2,3,4], Justin J. Greenlee[4], Amir N. Hamir[4], and M. Heather West Greenlee[3]

Abstract

Transmissible spongiform encephalopathies (TSEs) are a group of fatal neurodegenerative diseases characterized microscopically by spongiform lesions (vacuolation) in the neuropil, neuronal loss, and gliosis. Accumulation of the abnormal form of the prion protein (PrP^{Sc}) has been demonstrated in the retina of natural and non-natural TSE-affected hosts, with or without evidence of microscopically detectable retinal pathology. This study was conducted to investigate the effect of PrP^{Sc} accumulation on retinal neurons in a natural host lacking overt microscopic evidence of retinal degeneration by comparing the distribution of retinal cell type-specific markers in control and scrapie-affected sheep. In retinas with PrP^{Sc}-immunoreactivity, we observed disruption of the normal immunoreactivity patterns of the alpha isoform of protein kinase C (PKCα) and vesicular glutamate transporter 1 (VGLUT1), markers of retinal bipolar cells. Altered immunoreactivity was also observed for microtubule-associated protein 2 (MAP2), a marker of a subset of retinal ganglion cells, and glutamine synthetase (GS), a marker of Müller glia. These results demonstrate alterations of immunoreactivity patterns for proteins associated with specific cell types in retinas with PrP^{Sc} accumulation, despite an absence of microscopical evidence of retinal degeneration.

---

[1] Reprinted from the *Journal of Comparative Pathology*, 138:12-22, 2008, with permission from Elsevier Limited.
[2] Primary researcher and author.
[3] Department of Biomedical Sciences, Iowa State University, Ames, IA
[4] USDA National Animal Disease Center, Ames, IA.

Introduction

Transmissible spongiform encephalopathies (TSEs) are fatal neurodegenerative diseases presenting as inherited, sporadic, or infectious forms, with the accumulation of an abnormal form of prion protein (PrP^{Sc}) in the central nervous system (CNS) as their pathological underpinning. Examples of disorders in this group include kuru and Creutzfeldt-Jakob disease (CJD) in humans, scrapie in sheep and goats, bovine spongiform encephalopathy (BSE) in cattle, transmissible mink encephalopathy (TME) in mink, and chronic wasting disease (CWD) in cervids. The normal cellular isoform of the prion protein (PrP^{C}) exists as a GPI-anchored cell-surface protein, and is expressed primarily by cells of the CNS (Kretzschmar *et al.*, 1986; Moser *et al.*, 1995; Prusiner *et al.*, 1998).

The pathogenesis of TSEs is not well understood. Accumulation of PrP^{Sc} presumably occurs via conversion of native PrP^{C} into disease-associated PrP^{Sc} (Kocisko *et al.*, 1994; Bieschke *et al.*, 2004) ultimately resulting in neuronal cell death. In brains in which PrP^{Sc} accumulation is observed, neuronal cell populations appear to be differentially versus diffusely affected. Investigation into the pathogenesis of TSEs is further complicated when considering the effects of PrP^{Sc} accumulation in natural versus non-natural host species. For example, scrapie-affected sheep (natural host) with demonstrable retinal PrP^{Sc} accumulation do not appear to have associated major morphological changes in their retinas (Greenlee *et al.*, 2006), whereas retinas from scrapie-affected hamsters and mice (non-natural hosts) exhibit extensive photoreceptor degeneration (Buyukmihci *et al.*, 1980, 1982; Fraser et al., 1997; Hogan *et al.*, 1981).

Several attributes of the mammalian retina make it a useful model for studying TSE pathogenesis. The retina is a highly organized multicellular organ with a characteristic laminar structure consisting of alternating cellular and synaptic (plexiform) layers. There are five characteristic neuronal cell types and one retina-specific glial cell type, which can be easily distinguished from one another based on location and morphological characteristics, or with cell type-specific antibodies (Haverkamp and Wassle, 2000). Phototransduction (the process of converting light photons into neural signals) takes place in photoreceptor outer segments, the most sclerad portion of the neural retina. Photoreceptor-generated signals are then relayed vitreally to bipolar cells residing in the inner nuclear layer (INL), and then to

retinal ganglion cells in the ganglion cell layer (GCL), which project axons to centers of higher visual processing in the brain. Horizontal and amacrine cells play a modulatory role in this signaling pathway by way of their processes in the outer and inner plexiform layers, respectively. In retinas from scrapie-affected sheep, PrP^{Sc} accumulation is primarily observed in the inner plexiform layer (IPL), the layer of the retina where synaptic connections occur between retinal bipolar, amacrine, and ganglion cells, and the outer plexiform layer (OPL), where synaptic connections occur between horizontal, bipolar, and photoreceptor cells (Jeffrey *et al.*, 2001; Greenlee *et al.*, 2006). In both natural and non-natural host species with TSEs, the retina has been shown to accumulate PrP^{Sc} (Bradley, 1999; Foster *et al.*, 1999; Spraker *et al.*, 2002b; Valdez *et al.*, 2003; Head *et al.*, 2003, 2005; Hamir *et al.*, 2004, 2005; Kercher *et al.*, 2004; Hortells *et al.*, 2006; Greenlee *et al.*, 2006).

Although retinal PrP^{Sc} accumulation has been well documented, there is little information describing the effects of PrP^{Sc} accumulation on specific retinal cell types beyond cellular degeneration and loss as assessed by histopathology. To further investigate the effect of PrP^{Sc} accumulation on specific retinal cell types, the distribution of various cell type-specific markers in retinas from control and scrapie-affected adult sheep was examined. Morphological changes were demonstrated in some, but not all, retinal cell types in animals with retinal PrP^{Sc} accumulation. This is the first study of TSE in a natural host to describe changes in the morphology and/or protein expression patterns of specific retinal cells based on immunohistochemical examination of retinas with demonstrable PrP^{Sc} accumulation, but without obvious microscopical evidence of neuronal degeneration.

Materials and Methods

Animals and Tissue Preparation

The distribution of various cell type-specific markers in retinas from normal (scrapie-free) and scrapie–infected adult sheep was examined. Retinas examined here were collected as part of an earlier scrapie pathogenesis study (Hamir *et al.*, 2005). Suffolk sheep were inoculated via the intracerebral and oral routes at 4 months of age. Retinas examined in the present study were selected from sheep from the previous study euthanized at terminal stages of disease, and with immunoreactivity to PrP^{Sc} in brainstem and for which the retina was available. Entire globes with a segment of optic nerve of approximately 1-2 cm were

collected at necropsy. Connective tissue and muscle was removed from the area surrounding the optic nerve, and a scalpel was used to make a small slit through the connective tissue tunics at the junction of the cornea and sclera before immersion into 10% neutral buffered formalin. Tissues were allowed to fix for at least 3 weeks at which time a 5 mm thick vertical section from the caudal aspect of the globe containing retina and optic nerve were processed by routine histological methods and embedded into paraffin. Serial 4 µm sections from the retina were cut for immunohistochemistry (IHC). Retinas from at least two negative controls and six PrP^{Sc}-positive animals were used in the analysis of each retinal cell type-specific marker. All animal procedures had the approval of the National Animal Disease Center's Animal Care and Use Committee.

Immunohistochemistry

Slides were immunolabeled to detect PrP^{Sc} as previously described (Hamir *et al.*, 2004) using primary antisera containing monoclonal antibodies F89/160.5 (O'Rourke *et al.*, 1998) and F99/97.6.1 (Spraker *et al.*, 2002a) each at a concentration of 5 μM/ml. With each batch of slides labeled for PrP^{Sc}, serial sections of brainstem from a known positive sheep also were labeled for PrP^{Sc} to assess any variability between batches and additional slides were processed with the omission of the primary antibody to control for nonspecific labeling.

Sections immunolabeled to detect retinal cell type-specific antigens were deparaffinized in xylene and rehydrated in a decremental alcohol series. A proportion of the characterization of some of the retinal antigens in this study was performed on sections processed for double label analysis with PrP^{Sc}. Therefore, prior to IHC processing, all tissue sections (regardless of single- or double-label status) were subjected to a modified hydrated autoclaving pre-treatment protocol to enhance PrP^{Sc} detection. All sections were rinsed in 0.1 M citrate buffer, pH 6.2, and autoclaved at 100° C for 20 minutes in citrate buffer prior to IHC processing. All sections were then rinsed in potassium phosphate buffered solution (KPBS), pH 7.4, and incubated for two hours in blocking solution containing KPBS, 1% bovine serum albumin (BSA), 0.4% Triton X-100, and 1.5% normal donkey serum (NDS). Primary antibodies (see below) were diluted in the aforementioned blocking solution, and applied for overnight incubation at room temperature. On the following day, tissue sections were rinsed in KPBS with 0.2% Triton X-100 and incubated for two hours at room

temperature in the appropriate secondary antibody diluted 1:500 in KPBS with 1% BSA, 0.02% Triton X-100, and 1% NDS. Sections processed for fluorescence IHC were rinsed, incubated in 4',6-diamidine-2-phenylindole (DAPI; Molecular Probes, Carlsbad, CA) at room temperature for 5 minutes, and rinsed a final time in KPBS prior to being cover-slipped with Vectashield fluorescence mounting medium (Vector, Burlingame, CA).

Antibodies

Primary antibodies used in this study included the following: rabbit anti-glutamine synthetase (GS) (Sigma, St. Louis, MO), 1:10,000 dilution; rabbit anti-microtubule-associated protein 2 (MAP2) (Chemicon International, Inc., Temecula, CA), 1:100 dilution; rabbit anti-protein kinase C - alpha isoform (PKCα) (Sigma, St. Louis, MO); and guinea pig anti-vesicular glutamate transporter 1 (VGLUT1) (Chemicon International, Inc., Temecula, CA), 1:1000 dilution. Secondary antibodies used in this study included fluorescein isothiocyanate (FITC)-conjugated donkey anti-guinea pig IgG (Jackson Immunoresearch, West Grove, PA); or Alexa 488-conjugated donkey anti-rabbit IgG (Molecular Probes, Carlsbad, CA).

Examination of Tissue Sections

Tissue sections were examined with a Nikon Eclipse E800 fluorescent microscope (Nikon Corp., Tokyo, Japan). Images were captured using a Q-Imaging Retiga 1300 digital camera, and processed on a Macintosh G4 computer (Apple Computer, Cupertino, CA) using Improvision OpenLab 3.1.3. Figures were prepared using Adobe Photoshop CS Version 8.0 and Macromedia Freehand MX Version 11.0 for the Macintosh.

Results

To investigate the effect of PrP^{Sc} accumulation on retinal neurons, the distribution of retinal cell type-specific markers in normal and scrapie-infected sheep was examined. First, retinas from scrapie-positive sheep were assigned a grade of mild (+), moderate (++), or severe (+++) depending on the location and extent of retinal PrP^{Sc} accumulation (Fig. 2.1). Grades were assigned as follows: (+) = diffuse immunoreactivity of moderate intensity primarily confined to the inner and outer plexiform layers, but with occasional PrP^{Sc}-immunoreactive retinal ganglion cells; (++) = diffuse immunoreactivity of the inner and outer plexiform layers with multiple foci of immunoreactivity in the ganglion cell layer, inner

nuclear layer, and less frequently the outer nuclear layer; (+++) = intense immunoreactivity in the inner and outer plexiform layers with frequent and intense immunoreactivity in retinal ganglion cells, inner and outer nuclear layers, and photoreceptor outer segments with multiple small foci of immunoreactivity within the optic fiber layer (Fig. 2.1). This grading scheme was employed to categorize scrapie-positive animals in such a way that would allow us to determine if a correlation existed between the severity of retinal PrP^{Sc} accumulation and any observed changes in the distribution of retinal markers.

PKCα expression in ovine retinas with PrP^{Sc} accumulation

In the mammalian retina, antibodies directed against the alpha isoform of protein kinase C (PKCα) can be used as a marker of rod bipolar cells (Greferath *et al.*, 1990; Haverkamp and Wassle, 2000). Consistent with PKCα-immunoreactivity (-IR) in other species, PKCα-IR was observed in the cell bodies and processes of putative rod bipolar cells in control sheep retina (Fig. 2.2A). Immunoreactive cell bodies were observed at the scleral margin of the INL, with immunoreactive dendrites extending sclerad to the OPL. Uniformly projecting immunoreactive axons were observed extending through the INL into the IPL, where their terminals appeared as variably sized ovoid puncta of immunoreactivity along the vitreal margin of the IPL. In retinas of scrapie-affected animals, we observed differences in the pattern of PKCα-IR in axonal processes and terminals compared to control animals (Fig. 2.2B). Cell bodies in the INL continued to express moderate levels of PKCα, but a number of immunoreactive processes were observed terminating well sclerad to their appropriate level of termination at the vitreal border of the IPL (arrow in Fig. 2.2B). Synaptic terminals also appeared to have more of a branching pattern of PKCα-IR versus the relatively ordered puncta of immunoreactivity observed at the vitreal aspect of the IPL in control retina. The most pronounced alterations in PKCα-IR were observed in scrapie-affected animals with severe (+++) retinal PrP^{Sc} accumulation, but immunoreactivity in terminals also appeared more branched versus controls in retinas categorized as having mild (+) or moderate (++) PrP^{Sc} accumulation (data not shown).

VGLUT1-immunoreactivity in ovine retinas with PrP^{Sc} accumulation

Immunoreactivity for VGLUT1 has been demonstrated in glutamatergic terminals of photoreceptors in the OPL and bipolar cells in the IPL (Johnson *et al.*, 2003). In control

sheep retina, similar to other mammalian species, an intense band of coarse VGLUT1-IR was observed in the OPL in putative photoreceptor terminals, and as diffuse puncta of immunoreactivity throughout the IPL in presumed bipolar cell terminals (Fig. 2.2C). Larger puncta of VGLUT1-IR were numerous along the vitreal border of the IPL (arrows in Fig. 2.2C). No appreciable difference in the intensity or distribution of VGLUT1-IR between negative control retina and retinas where + to ++ PrP^{Sc} accumulation was detected. However, in retinas with +++ PrP^{Sc} accumulation, VGLUT1-IR was less intense and the larger puncta of immunoreactivity observed along the vitreal border of the IPL in control retina appeared less numerous (Fig. 2.2D).

Syntaxin 1- and ChAT-immunoreactivity patterns in ovine retinas with PrPSc accumulation

The distributions of two amacrine cell markers, syntaxin 1 and choline acetyltransferase (ChAT), were examined. In the retina, syntaxin 1-IR is present in the OPL where it is localized to horizontal cell processes (Hirano *et al.*, 2005), and in amacrine cells (Morgans *et al.*, 1996) which are the source of conventional synapses in the IPL. Antibodies directed against ChAT label a specific type of amacrine cell, the cholinergic amacrine cell (Voigt, 1986; Rodieck and Marshak, 1992; Haverkamp and Wassle, 2000). A difference in the distribution or intensity of Syntaxin1 or ChAT-IR between PrP^{Sc}-positive and negative control retinas (data not shown) was not observed.

MAP2 expression in ovine retinas with PrP^{Sc} accumulation

In the mature mammalian retina, antibodies against microtubule-associated protein 2 (MAP2) label a subpopulation of retinal ganglion cells and their processes in the IPL, some amacrine cells, and horizontal cells (Tucker and Matus, 1988; Okabe *et al.*, 1989). MAP2-IR in the retina of negative control sheep was primarily associated with a subset of larger ganglion cells and their dendritic processes in the IPL, which appeared as multifocal puncta of intense immunoreactivity distributed across the width of the layer (Fig. 2.3A). Low levels of MAP2-IR were also observed in the OPL, and occasionally in cell bodies at both the vitreal and scleral margin of the INL, likely a subpopulation of amacrine cells and horizontal cells, respectively. In PrP^{Sc}-positive retinas, the number of MAP2-positive cell bodies in the ganglion cell layer was decreased when compared to control retinas (Fig. 2.3B). Due to constraints of tissue availability consistent fields between retinal sections were not available

to permit enumeration of immunoreactive cells. However, this decrease (relative to controls) was quite striking on subjective examination, but only detected in +++ retinas. MAP2-IR in the INL and OPL of PrP^{Sc}-positive retina appeared similar to that of control retina.

GS-immunoreactivity in ovine retinas with PrP^{Sc} accumulation

In the mammalian retina, glutamine synthetase (GS) is expressed by Müller glia, the primary glial cell of the retina (Riepe and Norenburg, 1977; Haverkamp and Wassle, 2000). GS-IR in normal sheep retina (Fig. 2.3C) was observed in cell bodies located in the mid to vitreal half of the INL, and faintly in processes spanning the retina from the inner limiting membrane to the outer limiting membrane, consistent with previously described patterns of GS labeling of Müller glia in other mammalian species. Immunolabeling of Müller glia cell bodies was more intense in retinas with PrP^{Sc} accumulation versus control retinas. More prominent GS-IR was observed in the plexiform layers of all PrP^{Sc}-positive retinas examined, especially +++ retina (Fig. 2.3D).

Discussion

Appropriate cellular organization and connectivity are fundamental to proper function of the nervous system. The retina, with its laminated structure and extensively characterized cell types (the majority of which can be identified by predictable and distinct immunolabeling patterns), offers a model well suited for examining pathological changes of cellular organization. To date, the majority of retinal studies in naturally occurring and experimentally induced TSEs have focused on the distribution of PrP^{Sc} in the retina and/or the presence or absence of histological lesions indicative of retinal degeneration. Central to understanding the functional consequence of PrP^{Sc} accumulation in the retina is examination of alterations in normal retinal cell phenotypes that may occur as a result of PrP^{Sc} accumulation.

Although alterations in CNS neurons, such as synaptic loss, dendritic alterations, and enhanced expression of proapoptotic factors, have been reported in rodent models of TSEs prior to, or concomitant with, the appearance of obvious microscopic lesions (Belichenko et al., 2000; Jeffrey *et al.*, 2000; Jamieson *et al.*, 2001a,b; Cunningham *et al.*, 2003), evidence of similar disruption in natural hosts (e.g. sheep with scrapie) is lacking. In the current study, we have compared the distribution of various retinal cell type-specific markers in the retinas

from control and scrapie-affected sheep with demonstrable retinal PrP^{Sc} accumulation, which lack lesions consistent with retinal degeneration at the light microscopic level. Overall, the distribution of each of these markers in control sheep retina was consistent with previous immunohistochemical findings in other mammalian species. Of primary interest in this study, however, were observations of the disruption of normal immunoreactivity patterns of some, but not all, of these antigens in retinas with PrP^{Sc} accumulation. Figure 2.4 summarizes the retinal cellular changes that accompany PrP^{Sc} accumulation. We have demonstrated changes in the normal immunoreactivity patterns of PKCα, VGLUT1, MAP2, and GS in retinas from scrapie-positive sheep. Alterations in the distribution of the immunoreactivity patterns of these antigens present in bipolar, retinal ganglion and Müller glial cells respectively, were most evident in +++ retinas. Syntaxin 1 and ChAT immunolabeling of amacrine cells did not appear affected by retinal PrP^{Sc} accumulation.

PrP^{Sc} was detected primarily in the synaptic layers of all PrP^{Sc}-positive retinas examined (Fig. 2.1), but overt evidence of retinal cellular degeneration was not present on hematoxylin and eosin stained slides (previously reported by Greenlee *et al.*, 2006). Recently, a similar distribution of retinal PrP^{Sc} accumulation was described in sheep with naturally occurring scrapie (Hortells *et al.*, 2006), however the authors also reported associated histopathological lesions in some scrapie-affected sheep including loss of outer limitant layer definition, OPL atrophy, and inner and outer nuclear layer disorganization. This discrepancy may be due to differences in lesion interpretation in formalin fixed tissues, as the structural integrity of the retina is usually compromised to some degree by fixation in formalin. Also, each study examined retinas from different breeds of sheep (Rasa Aragonesa in Hortells et al., (2006), Suffolk in Greenlee et al. (2006)) with scrapie from different sources (natural infection in Hortells et al. (2006) versus experimental infection with a pooled inoculum in Greenlee et al. (2006)), raising the possibility that sheep background genetics or infecting scrapie strain(s) may contribute to the histopathological differences. Retinal lesions in some murine models of scrapie have been shown to be dependent on both the strain of mouse and strain of scrapie used (Foster *et al.*, 1986). Hortells et al. (2006) also assessed Müller glia by immunolabeling with glial fibrillary acidic protein (GFAP), but other cell types in the retina were not specifically evaluated. Our findings underscore the importance of examining the

morphology of retinal neurons beyond classical histological assessment in order to identify more subtle effects of PrP^{Sc} accumulation on specific retinal cell phenotypes that may be missed with hematoxylin and eosin staining.

Disruption of PKCα-IR was observed in rod bipolar cell processes within the IPL in retinas with PrP^{Sc} accumulation, suggesting these interneurons critical to the rod photoreceptor signaling pathway are affected by PrP^{Sc} accumulation. Our observations of a more prominent branching pattern of immunoreactivity at rod bipolar cell synaptic terminals in retinas with PrP^{Sc} accumulation versus control may indicate appropriate synaptic connectivity of these cells has been disrupted and they are responsively sprouting processes in an effort to re-establish proper circuitry. Axonal and synaptic pathology have been described in naturally occurring (Liberski and Budka, 1999; Ferrer *et al.*, 2000) and experimental (Jeffrey *et al.*, 1995; Siso *et al.*, 2002) TSEs. The retina, like other CNS tissues, exhibits extensive remodeling in response to degenerative disease (Jones and Marc, 2005). PKCα-immunoreactive processes were also observed terminating sclerad to the vitreal border of the IPL in retinas with +++ PrP^{Sc} accumulation, suggesting that perhaps these cells are retracting their axons in response to PrP^{Sc} or to loss of their appropriate targets. Alterations in PKCα-IR seemed to correlate with the degree of PrP^{Sc} accumulation to some degree, as 'retracted' processes were not observed in + or ++ retina.

Another observed change in the IPL of retinas with PrP^{Sc} accumulation was a decrease in VGLUT1-IR, especially along the vitreal border of the IPL where more prominent puncta of VGLUT1-IR are normally found. VGLUT1 is localized to photoreceptor and bipolar cell terminals in the retina. Based on the normal anatomical location of rod bipolar cell terminals and their appearance when labeled for PKCα, it is feasible that the observed decrease in VGLUT1-IR at the vitreal border of the IPL represents a decrease in the number of rod bipolar cell terminals. Taken together, these data suggest rod bipolar cells are one specific cell type affected by the accumulation of PrP^{Sc} in the retina of sheep with scrapie, raising the possibility that rod-mediated vision may be impaired in these animals.

Retinal ganglion cell axons comprise the optic nerve and relay visual signals from the retina to centers of higher visual processing in the brain. A qualitative decrease in the number of MAP2-positive cells in the GCL of retinas with +++ PrP^{Sc} accumulation was

observed, suggesting either down-regulation of MAP2 expression by affected cells, or loss of MAP2-positive GCs. Interestingly, PrP^{Sc} was detected in occasional GCs in retinas with mild (+) PrP^{Sc} accumulation, but a decrease in the number of MAP2-positive cells was not detected in these or ++ retinas. Russelakis-Carneiro *et al.* (1999) demonstrated retinal ganglion cell degeneration in mice intraocularly inoculated with the ME7 strain of scrapie, but not until the terminal stages of disease, suggesting (at least in that model) retinal GCs may be somewhat resistant to the adverse effects of PrP^{Sc} versus other cell types. In contrast, Hortells *et al*. (2006) recently reported an absence of histological lesions in the GCL in sheep with naturally occurring scrapie. In the current study, retinal ganglion cells appeared normal histologically, and abnormalities were not observed until ganglion cell specific labeling was used, emphasizing the importance of examining TSE-associated retinal pathology using several techniques.

Antibodies against amacrine cell markers were similar between control and PrP^{Sc}-positive retina, suggesting the overall organization of amacrine cells may be intact in retinas with PrP^{Sc} accumulation. Taken together with the aforementioned data, these observations also offer evidence for a type of selective cellular disruption in the retinas of sheep with scrapie versus generalized pan-retinal degeneration.

Müller glia have long been proposed to play a supportive role in the retina, but have also been assigned potential roles in cellular regeneration (Garcia and Vecino, 2003) and modulation of synaptic transmission (Newman, 2004). As part of their neuroprotective function, Müller glia express glutamine synthetase, which, by converting glutamate to glutamine, prevents glutamate-induced excitotoxicity. Increased GS-IR was observed in retinas with PrP^{Sc} accumulation, suggesting GS expression may be up-regulated in these cells in response to increased extracellular glutamate levels, and/or GS-IR may be more prominent owing to generalized cellular hypertrophy of Müller glia in response to retinal stress. In addition to cellular hypertrophy, Müller glia also up-regulate their expression of GFAP in response to retinal injury (Ekstrom *et al.*, 1988). Increased GFAP expression has recently been demonstrated in the retinas of sheep (Hortells *et al.*, 2006; Greenlee *et al.*, 2006) and transgenic mice (Kercher *et al.*, 2004) infected with scrapie. These results suggest Müller

glia are affected by retinal PrP^{Sc} accumulation, but may be responding appropriately to said stress.

An additional interesting observation made while examining the various immunolabeling patterns in this study, especially syntaxin 1 and VGLUT1, which are diffusely distributed across the IPL, was that the IPL in retinas with PrP^{Sc} accumulation was subjectively assessed as thinner versus that of control retina. This discrepancy in IPL thickness cannot be quantified, however, due to our inability to examine consistent regions between retinal sections, but when the relative thickness of other retinal layers (e.g. ONL, INL) is compared, these layers appear very similar, suggesting selective thinning of the IPL may be occurring in PrP^{Sc}-positive retina.

We have taken an initial step in a series of interesting studies that could be performed using the retina as a model to study TSE pathogenesis. Observations of increased GFAP expression despite a lack of overt retinal pathology in the retinas examined in this study (described previously by Greenlee *et al.*, 2006) raise the possibility that active retinal pathology is present, but that it is occurring at a level that is not causing severe photoreceptor degeneration or morphological disruption of other retinal neurons, as has been observed in earlier studies using non-natural experimental hosts (Buyukmihci et al., 1980, 1982; Hogan et al., 1981). Our findings support this possibility and demonstrate disruption of specific retinal neurons that are crucial for visual signals to make it from photoreceptor to brain. Since much is known about the electrophysiological properties of the retina, it is possible to study relationships between specific morphological changes and electrophysiological dysfunction. Our observations are a necessary first step in understanding functional disruptions in the retinas of these TSE-affected natural hosts, and will provide guidance for future investigations into the effects of PrP^{Sc} on retinal morphology and function.

Acknowledgments

The authors thank Joe Lesan, Dennis Orcutt, and Martha Church for technical assistance and immunohistochemical staining. This study was supported by Specific Cooperative Agreement #58-3625-5-114 with the Agricultural Research Service, USDA.

References

Belichenko, P.V., Brown, D., Jeffrey, M., Fraser, J.R., (2000). Dendritic and synaptic alterations of hippocampal pyramidal neurons in scrapie-infected mice. *Neuropathology Applied Neurobiology*, **26**, 143-149.

Bieschke, J., Weber, P., Sarafoff, N., Beekes, M., Giese, A. and Kretzschmar, H. (2004). Autocatalytic self-propagation of misfolded prion protein. *Proceedings of the National Academy of Sciences of the U S A,* **101,** 12207-12211.

Bradley, R. (1999). BSE transmission studies with particular reference to blood. *Developments in Biological Standardization,* **99,** 35-40.

Buyukmihci, N., Goehring-Harmon, F. and Marsh, R. F. (1982). Photoreceptor degeneration preceding clinical scrapie encephalopathy in hamsters. *Journal of Comparative Neurology,* **205,** 49-54.

Buyukmihci, N., Rorvik, M. and Marsh, R. F. (1980). Replication of the scrapie agent in ocular neural tissues. *Proceedings of the National Academy of Sciences of the U S A,* **77,** 1169-1171.

Cunningham, C., Deacon, R., Wells, H., Boche, D., Waters, S., Picanco Diniz, C., Scott, H., Rawlins, J.N.P., Perry, V.H. (2003). Synaptic changes characterize early behavioural signs in the ME7 model of murine prion disease. *European Journal of Neuroscience*, **17**, 2147-2155.

Ekstrom, P., Sanyal, S., Narfstrom, K., Chader, G. J. and van Veen, T. (1988). Accumulation of glial fibrillary acidic protein in Müller radial glia during retinal degeneration. *Investigative Ophthalmology and Visual Science,* **29,** 1363-1371.

Ferrer, I., Puig, B., Blanco, R. and Marti, E. (2000). Prion protein deposition and abnormal synaptic protein expression in the cerebellum in Creutzfeldt-Jakob disease. *Neuroscience,* **97,** 715-726.

Foster, J., Farquhar, C., Fraser, J. and Somerville, R. (1999). Immunolocalization of the prion protein in scrapie affected rodent retinas. *Neuroscience Letters,* **260,** 1-4.

Fraser, J.R., Brown, J., Bruce M.E., Jeffrey, M. (1997). Scrapie-induced neuron loss is reduced by treatment with basic fibroblast growth factor. *Neuroreport*, **8**, 2405-2409.

Garcia, M. and Vecino, E. (2003). Role of Müller glia in neuroprotection and regeneration in the retina. *Histology and Histopathology,* **18,** 1205-1218.

Greenlee, J. J., Hamir, A. N., West Greenlee, M. H. (2006). Abnormal prion accumulation associated with retinal pathology in experimentally inoculated scrapie-affected sheep. *Veterinary Pathology*, **43**, 733-739.

Greferath, U., Grunert, U. and Wassle, H. (1990). Rod bipolar cells in the mammalian retina show protein kinase C-like immunoreactivity. *Journal of Comparative Neurology,* **301,** 433-442.

Hamir, A. N., Miller, J. M., Cutlip, R. C., Kunkle, R. A., Jenny, A. L., Stack, M. J., Chaplin, M. J. and Richt, J. A. (2004). Transmission of sheep scrapie to elk (*Cervus elaphus nelsoni*) by intracerebral inoculation: final outcome of the experiment. *Journal of Veterinary Diagnostic Investigation,* **16,** 316-321.

Hamir, A. N., Kunkle, R. A., Richt, J. A., Miller, J. M., Cutlip, R. C. and Jenny, A. L. (2005). Experimental transmission of sheep scrapie by intracerebral and oral routes to genetically susceptible Suffolk sheep in the United States. *Journal of Veterinary Diagnostic Investigation,* **17,** 3-9.

Haverkamp, S. and Wassle, H. (2000). Immunocytochemical analysis of the mouse retina. *Journal of Comparative Neurology,* **424,** 1-23.

Head, M. W., Northcott, V., Rennison, K., Ritchie, D., McCardle, L., Bunn, T. J., McLennan, N. F., Ironside, J. W., Tullo, A. B. and Bonshek, R. E. (2003). Prion protein accumulation in eyes of patients with sporadic and variant Creutzfeldt-Jakob disease. *Investigative Ophthalmology and Visual Science,* **44,** 342-346.

Head, M. W., Peden, A. H., Yull, H. M., Ritchie, D. L., Bonshek, R. E., Tullo, A. B. and Ironside, J. W. (2005). Abnormal prion protein in the retina of the most commonly occurring subtype of sporadic Creutzfeldt-Jakob disease. *British Journal of Ophthalmology,* **89,** 1131-1133.

Hirano, A. A., Brandstatter, J. H. and Brecha, N. C. (2005). Cellular distribution and subcellular localization of molecular components of vesicular transmitter release in horizontal cells of rabbit retina. *Journal of Comparative Neurology,* **488,** 70-81.

Hogan, R. N., Baringer, J. R. and Prusiner, S. B. (1981). Progressive retinal degeneration in scrapie-infected hamsters: a light and electron microscopic analysis. *Laboratory Investigation,* **44,** 34-42.

Hortells, P., Monzon, M., Monleon, E., Acin, C., Vargas, A., Bolea, R., Lujan, L., Badiola, J.J. (2006). Pathological findings in retina and visual pathways associated to natural scrapie in sheep. *Brain Research*, **1108**, 188-194.

Jamieson, E., Jeffrey, M., Ironside, J.W., Fraser, J.R. (2001a). Apoptosis and dendritic dysfunction precede prion protein accumulation in 87V scrapie. *Neuroreport*, **12**, 2147-2153.

Jamieson, E., Jeffrey, M., Ironside, J.W., Fraser, J.R. (2001b). Activation of Fas and caspase 3 precedes PrP accumulation in 87V scrapie. *Neuroreport*, **12**, 3567-3572.

Jeffrey, M., Fraser, J. R., Halliday, W. G., Fowler, N., Goodsir, C. M. and Brown, D. A. (1995). Early unsuspected neuron and axon terminal loss in scrapie-infected mice revealed by morphometry and immunocytochemistry. *Neuropathology and Applied Neurobiology,* **21,** 41-49.

Jeffrey, M., Halliday, W.G., Bell, J., Johnston, A.R., Macleod, N.K., Ingham, C., Sayers, A.R., Brown, D.A., Fraser, J.R. (2000). Synapse loss associated with abnormal PrP precedes neuronal degeneration in the scrapie-infected murine hippocampus. *Neuropathology and Applied Neurobiology*, **26**, 41-54.

Jeffrey, M., Martin, S., Thomson, J. R., Dingwall, W. S., Begara-McGorum, I., Gonzalez, L. (2001). Onset and distribution of tissue PrP accumulation in scrapie-affected Suffolk sheep as demonstrated by sequential necropsies and tonsillar biopsies. *Journal of Comparative Pathology,* **125**, 48-57.

Johnson, J., Tian, N., Caywood, M. S., Reimer, R. J., Edwards, R. H. and Copenhagen, D. R. (2003). Vesicular neurotransmitter transporter expression in developing postnatal rodent retina: GABA and glycine precede glutamate. *Journal of Neuroscience,* **23,** 518-529.

Jones, B. W. and Marc, R. E. (2005). Retinal remodeling during retinal degeneration. *Experimental Eye Research,* **81,** 123-137.

Kercher, L., Favara, C., Chan, C. C., Race, R. and Chesebro, B. (2004). Differences in scrapie-induced pathology of the retina and brain in transgenic mice that express

hamster prion protein in neurons, astrocytes, or multiple cell types. *American Journal of Pathology,* **165,** 2055-2067.

Kocisko, D. A., Come, J. H., Priola, S. A., Chesebro, B., Raymond, G. J., Lansbury, P. T. and Caughey, B. (1994). Cell-free formation of protease-resistant prion protein. *Nature,* **370,** 471-474.

Kretzschmar, H. A., Prusiner, S. B., Stowring, L. E. and DeArmond, S. J. (1986). Scrapie prion proteins are synthesized in neurons. *American Journal of Pathology,* **122,** 1-5.

Liberski, P. P. and Budka, H. (1999). Neuroaxonal pathology in Creutzfeldt-Jakob disease. *Acta Neuropathologica (Berl),* **97,** 329-334.

Morgans, C. W., Brandstatter, J. H., Kellerman, J., Betz, H. and Wassle, H. (1996). A SNARE complex containing syntaxin 3 is present in ribbon synapses of the retina. *Journal of Neuroscience,* **16,** 6713-6721.

Moser, M., Colello, R. J., Pott, U. and Oesch, B. (1995). Developmental expression of the prion protein gene in glial cells. *Neuron,* **14,** 509-517.

Newman, E. A. (2004). Glial modulation of synaptic transmission in the retina. *Glia,* **47,** 268-274.

O'Rourke, K. I., Baszler, T. V., Miller, J. M., Spraker, T. R., Sadler-Riggleman, I. and Knowles, D. P. (1998). Monoclonal antibody F89/160.1.5 defines a conserved epitope on the ruminant prion protein. *Journal of Clinical Microbiology,* **36,** 1750-1755.

Okabe, S., Shiomura, Y. and Hirokawa, N. (1989). Immunocytochemical localization of microtubule-associated proteins 1A and 2 in the rat retina. *Brain Research,* **483,** 335-346.

Prusiner, S. B., Scott, M. R., DeArmond, S. J. and Cohen, F. E. (1998). Prion protein biology. *Cell,* **93,** 337-348.

Riepe, R. E. and Norenburg, M. D. (1977). Müller cell localization of glutamine synthetase in rat retina. *Nature,* **268,** 654-655.

Rodieck, R. W. and Marshak, D. W. (1992). Spatial density and distribution of choline acetyltransferase immunoreactive cells in human, macaque, and baboon retinas. *Journal of Comparative Neurology,* **321,** 46-64.

Russelakis-Carneiro, M., Betmouni, S. and Perry, V. H. (1999). Inflammatory response and retinal ganglion cell degeneration following intraocular injection of ME7. *Neuropathology and Applied Neurobiology,* **25,** 196-206.

Siso, S., Puig, B., Varea, R., Vidal, E., Acin, C., Prinz, M., Montrasio, F., Badiola, J., Aguzzi, A., Pumarola, M. and Ferrer, I. (2002). Abnormal synaptic protein expression and cell death in murine scrapie. *Acta Neuropathologica (Berl),* **103,** 615-626.

Spraker, T. R., O'Rourke, K. I., Balachandran, A., Zink, R. R., Cummings, B. A., Miller, M. W. and Powers, B. E. (2002a). Validation of monoclonal antibody F99/97.6.1 for immunohistochemical staining of brain and tonsil in mule deer (*Odocoileus hemionus*) with chronic wasting disease. *Journal of Veterinary Diagnostic Investigation,* **14,** 3-7.

Spraker, T. R., Zink, R. R., Cummings, B. A., Wild, M. A., Miller, M. W. and O'Rourke, K. I. (2002b). Comparison of histological lesions and immunohistochemical staining of proteinase-resistant prion protein in a naturally occurring spongiform encephalopathy of free-ranging mule deer (*Odocoileus hemionus*) with those of chronic wasting disease of captive mule deer. *Veterinary Pathology,* **39,** 110-119.

Tucker, R. P. and Matus, A. I. (1988). Microtubule-associated proteins characteristic of embryonic brain are found in the adult mammalian retina. *Developmental Biology,* **130,** 423-434.

Valdez, R. A., Rock, M. J., Anderson, A. K. and O'Rourke, K. I. (2003). Immunohistochemical detection and distribution of prion protein in a goat with natural scrapie. *Journal of Veterinary Diagnostic Investigation,* **15,** 157-162.

Voigt, T. (1986). Cholinergic amacrine cells in the rat retina. *Journal of Comparative Neurology,* **248,** 19-35.

Figure Legends

Figure 1. PrP^{Sc} immunoreactivity (-IR) in the retinas of scrapie-infected sheep. **A:** In animals with retinal PrP^{Sc} accumulation categorized as mild (+) in our study, PrP^{Sc}-IR is present in both the IPL and OPL, and in occasional ganglion cells (arrow). **B:** In addition to PrP^{Sc}-IR in both plexiform layers and ganglion cells, punctate PrP^{Sc}-IR was also detected in the INL in animals with moderate (++) retinal PrP^{Sc} accumulation. **C:** In the most severely affected retinas examined (+++), PrP^{Sc}-IR was detectable in all retinal layers, including photoreceptor inner segments (arrows). OS, outer segments; ONL, outer nuclear layer; OPL, outer plexiform layer; INL, inner nuclear layer; IPL, inner plexiform layer; GCL, ganglion cell layer. Scale bars = 20μm.

Figure 2. Distribution of the alpha isoform of protein kinase C (PKCα) and vesicular glutamate transporter 1 (VGLUT1) in negative control and PrP^{Sc}-positive sheep retina. **A:** PKCα-IR was detected in cell bodies and processes of putative rod bipolar cells in normal sheep retina. **B:** Immunoreactive axonal processes in retinas with severe PrP^{Sc} accumulation appeared to branch more extensively and occasionally terminate sclerad to the vitreal border of the IPL (arrow) versus PKCα-immunoreactive processes in control retina. **C:** In control retinas, an intense band of coarse VGLUT1-IR was observed in the OPL. Small puncta of VGLUT1-IR were observed throughout the IPL, and a population of larger puncta was discernable at the vitreal border of the IPL. **D:** VGLUT1-IR appeared less intense in the plexiform layers of retinas with PrP^{Sc} accumulation, especially along the vitreal border of the IPL. Fewer larger puncta (arrows) were detected in this region versus control retina. OS,

outer segments; ONL, outer nuclear layer; OPL, outer plexiform layer; INL, inner nuclear layer; IPL, inner plexiform layer; GCL, ganglion cell layer. Scale bars = 10μm.

Figure 3. Distribution of microtubule-associated protein 2 (MAP2) and glutamine synthetase (GS) in the retina of negative control and scrapie-infected sheep. **A:** The majority of MAP2-IR was observed in a subset of cells in the GCL (asterisks) and their dendrites in the IPL. Immunoreactive processes could occasionally be seen projecting into the IPL (arrow). Faint MAP2-IR was observed in the OPL. **B:** Fewer MAP2-positive cells (asterisks) were observed in the GCL of retinas with +++ PrP^{Sc} accumulation. **C:** In control retinas, GS-IR was detected in cell bodies and processes of putative Müller glia, and at the inner (arrows) and outer (not shown) limiting membranes. **D:** GS-IR was observed in PrP^{Sc}-positive retina in a pattern similar to that of control retina, but more intense –IR was detected in Müller glia cell bodies and both plexiform layers. OS, outer segments; ONL, outer nuclear layer; OPL, outer plexiform layer; INL, inner nuclear layer; IPL, inner plexiform layer; GCL, ganglion cell layer; OFL, optic fiber layer. Scale bars = 10μm.

Figure 4. Schematic representation of normal retinal architecture. Light signals transmitted from rod photoreceptors are relayed to rod bipolar cells, which then conduct signals to retinal ganglion cells. Horizontal and amacrine cells function in modulating this signaling pathway. The 'X's indicate in which cell types we observed disrupted immunolabeling patterns in PrP^{Sc}-positive retina. Immunolabeling patterns specific to photoreceptors and horizontal cells were not examined. OS, outer segments; ONL, outer nuclear layer; OPL, outer plexiform layer; INL, inner nuclear layer; IPL, inner plexiform layer; GCL, ganglion cell layer; OFL, optic fiber layer.

Figure 1.

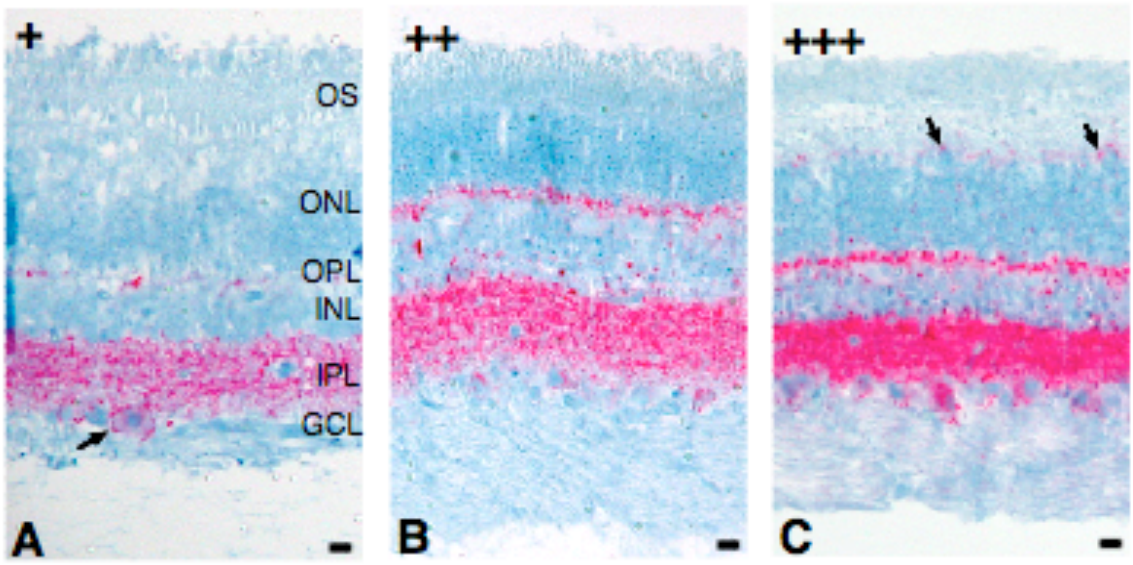

Figure 2.

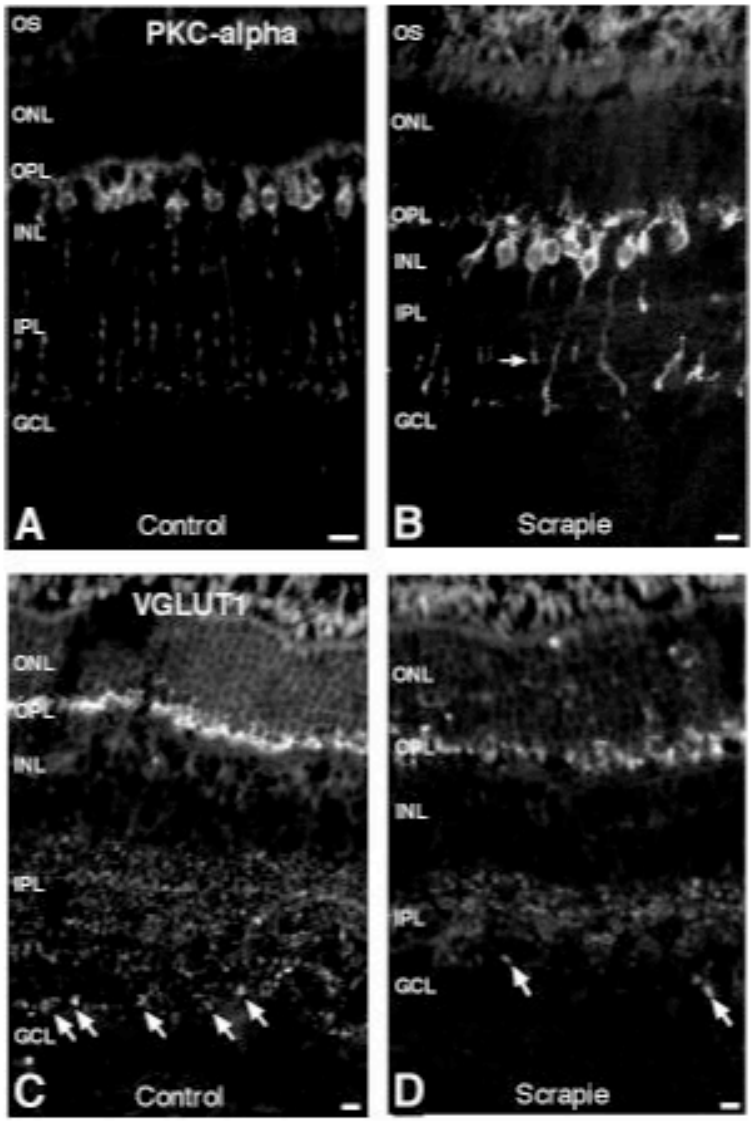
PKC-alpha
OS
ONL
OPL
INL
IPL
GCL
A
Control
B
Scrapie
VGLUT1
C
Control
D
Scrapie

Figure 3.

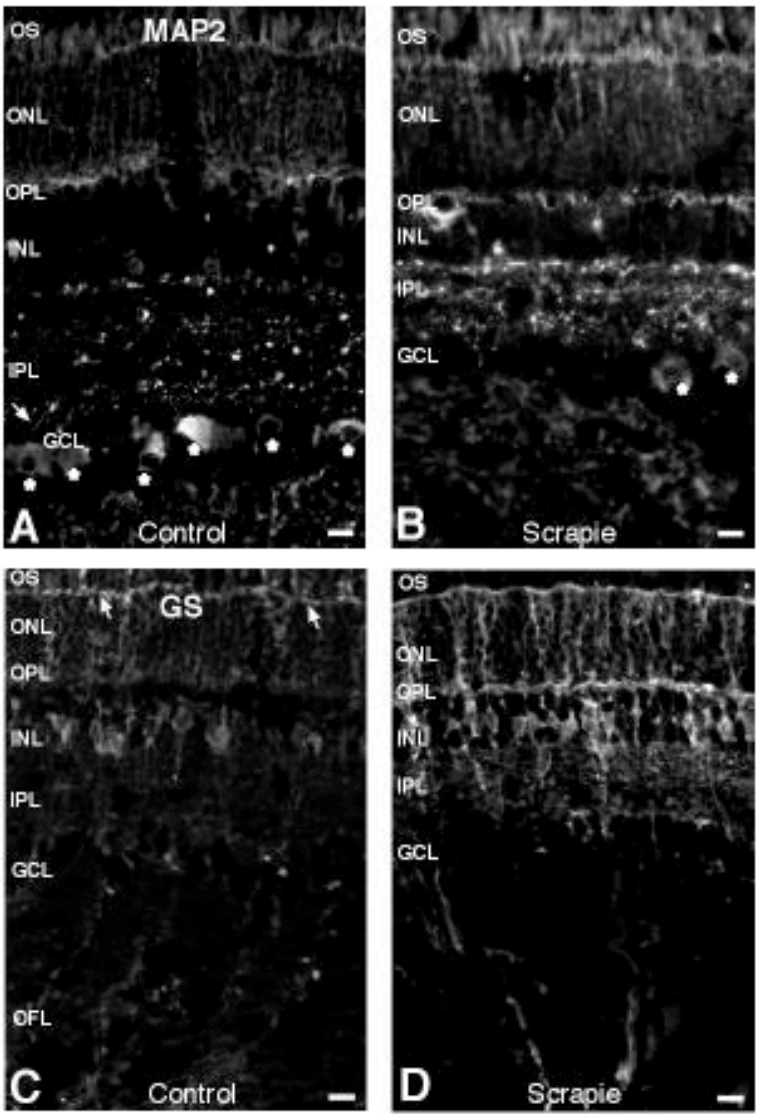
MAP2
OS
ONL
OPL
INL
IPL
GCL
A
Control
B
Scrapie
GS
OFL
C
Control
D
Scrapie

Figure 4.

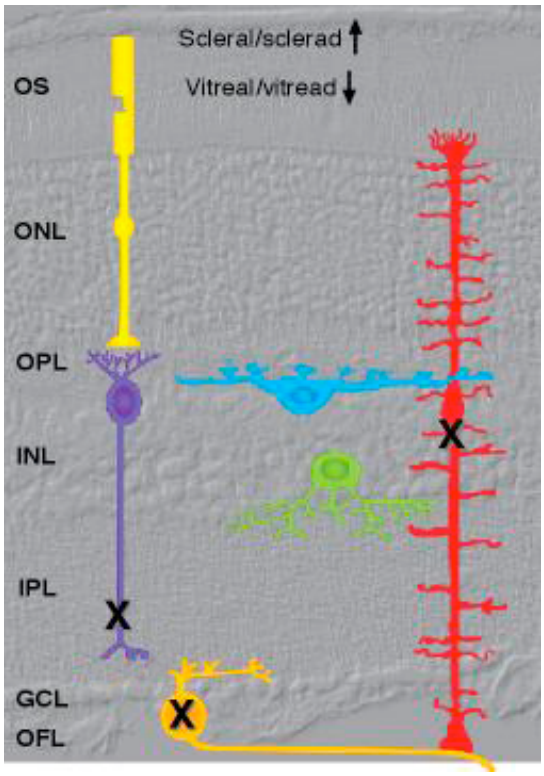
Scleral/sclerad
Vitreal/vitread
OS
ONL
OPL
INL
IPL
GCL
OFL
X
X
X

CHAPTER 3. RETINAL FUNCTION AND MORPHOLOGY ARE ALTERED IN CATTLE EXPERIMENTALLY INFECTED WITH TRANSMISSIBLE MINK ENCEPHALOPATHY

A paper to be submitted to *Nature*

Jodi D. Smith[1,2,3], Justin J. Greenlee[2], Amir N. Hamir[2], Juergen A. Richt[2], and M. Heather West Greenlee[3]

Abstract

Transmissible spongiform encephalopathies (TSEs) are a group of diseases, which result in progressive and invariably fatal neurological disease in both animals and humans. TSEs are characterized by the accumulation of an abnormal protease resistant form of the prion protein in the central nervous system. Abnormal prion protein has been reported in the retina of TSE affected cattle, but the specific effect(s) of abnormal prion protein on retinal morphology and function have not been assessed. The objective of this study was to identify and characterize potential functional and morphologic abnormalities in the retinas of cattle infected with a bovine-adapted isolate of transmissible mink encephalopathy (TME). We have examined retinas from non-inoculated and TME-inoculated Holstein steers with electroretinography and immunohistochemistry. Here we show altered retinal function in preclinical TME-infected cattle as evidenced by prolonged implicit time of the electroretinogram b-wave. We also demonstrate altered patterns of immunoreactivity for markers of rod bipolar cells and Müller glia in the retinas of these cattle at the time of euthanasia due to clinical deterioration. This study is the first to identify both functional and morphologic alterations in the retinas of TSE-infected cattle, and provides support for electroretinography to potentially serve as a new screening strategy for TSEs in cattle.

Introduction

Transmissible spongiform encephalopathies (TSEs) are invariably fatal neurological diseases, which affect a number of mammalian species. Central nervous system accumulation of an abnormal form of the cellular prion protein (PrP^{Sc}) and spongiform

---

[1] Primary researcher and author.
[2] USDA National Animal Disease Center, Ames, IA.
[3] Department of Biomedical Sciences, Iowa State University, Ames, IA.

change are characteristic of these diseases. Transmission of most infectious forms of TSE is believed to occur via ingestion of PrP^{Sc}-contaminated material. Natural transmission of bovine spongiform encephalopathy (BSE or 'mad cow disease') to humans is believed to have occurred, resulting in the variant form of Creutzfeldt-Jakob disease (vCJD).[1,2] Interspecies transmission of other TSEs has been accomplished experimentally. Transmissible mink encephalopathy (TME), a TSE which naturally occurs in mink, has been experimentally transmitted to cattle via the intracerebral route[3,4] with resulting histopathology reportedly indistinguishable from BSE.[4] Unfortunately, current methods for detecting TSEs in cattle are limited to postmortem analyses, creating a need for ante-mortem screening and diagnostic tools.

The retina is a thin, highly organized piece of neural tissue lining the posterior aspect of the eye, and is responsible for initiating vision by transducing light into neural signals. PrP^{Sc} has been demonstrated in the retinas of a number of TSE-affected species,[5-13] including cattle,[4] and accumulates primarily within the plexiform (synaptic) layers of the retina. Currently, the effect(s) of PrP^{Sc} accumulation on specific retinal cell types in cattle is unknown. Some retinal cell subtypes in sheep with scrapie are affected by PrP^{Sc},[14] suggesting that retinal function could be altered in prion-infected livestock. Electroretinography is a noninvasive tool used to evaluate retinal function. Reports on the use of electroretinography to evaluate retinal function in TSE-infected animals and humans are limited,[15-17] and to date, studies applying this methodology to TSE-infected cattle have not been reported.

This study investigated the effects of TSE infection on bovine retina using electroretinography and immunohistochemistry. Here we report that the electroretinogram b-wave is altered in TME-infected cattle prior to clinical signs of disease, and that there are subtle histologic and immunohistochemical differences between the retinas of TME-affected and non-inoculated cattle.

Results

Electroretinography

To evaluate retinal function in TME-infected cattle, we compared electroretinograms (ERG) between non-inoculated control and TME-inoculated cattle. All five TME-infected cattle were tested prior to the onset of clinical signs of disease (at 12.5, 13.5, and 14.5 months post-inoculation), and two of five were tested at 18.5 months post-inoculation, which was 1 or 2.5 weeks prior to euthanasia due to clinical deterioration. All TME-infected cattle were displaying some degree of neurological dysfunction, identified via extensive neurological examination, at approximately 15 months post-inoculation (Francisco Vargas, personal communication). Both dark- (scotopic) and light- (photopic) adapted tests were performed, and the resulting electroretinogram (ERG) b-wave amplitude and implicit time were analyzed. Representative ERGs from a non-inoculated control and a preclinical TME-infected animal are shown in Figure 1. A statistically significant increase in b-wave implicit time in TME-infected cattle was shown at all preclinical time points under all testing conditions, with the exception of test 2 at the earliest time point (Fig. 2). A significant difference in b-wave amplitude was, however, not observed at any preclinical time point. Analysis of b-wave values from two of the five TME-infected cattle during the clinical stage of disease demonstrated decreased average b-wave amplitude and prolonged implicit time under scotopic conditions relative to controls (Fig. 2, table). B-wave amplitude was decreased but implicit time was not prolonged under photopic conditions.

Histopathology and PrP^{Sc} distribution

To evaluate the morphologic effects of TSE infection on the retina of cattle, we examined retinas from cattle clinically affected with TME using standard histologic techniques and immunohistochemistry. Examination of hematoxylin and eosin stained sections (Fig. 3a,b) revealed mild pathologic change. Evidence of spongiform change was observed within the inner plexiform layer (IPL) of TME-affected cattle, but not in controls (arrows Fig. 3b). Cell density within the ganglion cell layer (GCL) differed between the two groups with controls having an average of 114 nuclei per five 40x fields versus 44 nuclei per five 40x fields in TME-affected cattle. Immunoreactivity (IR) for PrP^{Sc} was detected in the

retinas of all TME cattle, and was localized primarily to the synaptic layers and the cytoplasm of retinal ganglion cells (Fig. 3d).

Immunohistochemistry

Antibodies directed against retinal cell types contributing to the ERG b-wave (rod bipolar cells and Müller glia) were used to examine these cell populations in cattle clinically affected with TME. In control retinas, immunoreactivity for the alpha isoform of protein kinase C (PKCα) was present in rod bipolar cells (Fig. 4a). Relative to controls, PKCα-IR in TME-affected cattle appeared less uniform across the outer plexiform layer (OPL), and there were fewer distinct, large, ovoid puncta at the level of rod bipolar cell terminals (Fig. 4e). Glutamatergic photoreceptor and bipolar cell terminals were immunoreactive for vesicular glutamate transporter 1 (VGLUT1) in control retinas (Fig. 4b). Compared to controls, VGLUT1-IR in retinas from TME-affected cattle was less obviously associated with larger bipolar cell terminals along the vitreal border of the IPL (Fig. 4f). Müller glia were labeled in their entirety by antibodies against glutamine synthetase (GS) in both control and TME-affected retinas (Fig. 4c,g), but subtly higher levels of GS-IR were observed in the processes of Müller glia, specifically the portion coursing through the IPL, in TME-affected cattle versus controls. Immunoreactivity for glial fibrillary acidic protein (GFAP) was detected in the optic fiber layer of both control and TME-affected cattle, but markedly fewer and less prominent immunoreactive radial processes were observed in control retina compared to TME-affected retina (Fig. 4d,h).

Discussion

In this study, we examined both functional and morphologic consequences of PrP^{Sc} accumulation on the bovine retina using electroretinography and immunohistochemistry. Our electroretinography results demonstrate altered retinal function in TME-inoculated cattle prior to clinical disease. This is the first report of a detectable change in a neurophysiological parameter in a TSE-infected animal prior to clinical signs of disease. Further, we demonstrate morphologic abnormalities in the retinas of these cattle during clinical stages of disease, which are consistent with the observed changes in function.

Several lines of evidence suggest the rod bipolar cell is primarily responsible for generating the ERG b-wave, while Müller glia are currently regarded as a lesser participant.[18]

Our results demonstrate prolonged ERG b-wave implicit time in preclinical cattle. We also demonstrate altered immunolabeling patterns of rod bipolar cell markers (PKCα[19], VGLUT1[20]) and Müller glia markers (GS[19], GFAP[7]) in clinically affected cattle. Taken together, these data indicate PrP^{Sc}-induced pathology may be occurring in the retina prior to clinical disease, and especially affecting rod bipolar cells and Müller glia. Alteration of the b-wave in TME-inoculated cattle, which have PrP^{Sc} accumulation in synaptic layers at clinical stages of disease, suggests synaptic transmission in the retina may be altered, even at preclinical stages of disease. This could indicate early impairment or loss of functional normal cellular prion protein (PrP^{C}), or disruption of synapses or synaptic proteins secondary to PrP^{Sc} accumulation. Cellular stress may also play a role, as antioxidant properties have been ascribed to PrP^{C},[21,22] and PrP^{C} has been implicated in transducing neuroprotective signals in retinal explants.[23] Prolonged b-wave implicit time for both scotopic and photopic tests suggests both rod and cone photoreceptor pathways are affected.

Human CJD patients have been reported to exhibit various symptoms of visual disturbance.[24] Similar to ERG reports from CJD-affected patients,[16, 17] b-wave amplitude was decreased in two clinically affected TME cattle. This observed decrease in b-wave amplitude during the clinical, versus the preclinical, stage is likely a function of the extent of PrP^{Sc} accumulation in the retina and its associated pathology. For the photopic ERG, average b-wave implicit time for these two clinically affected cattle was similar to the mean control value. This observation was not consistent with our findings during the preclinical period, but could be due to the small sample size and relatively small duration of the photopic response.

We have demonstrated altered retinal function in TME-infected cattle prior to clinical disease. Further studies are needed to establish whether correlative changes in retinal cellular morphology are present during this preclinical period, and whether similar functional alterations are present in cattle with their naturally occurring TSE, bovine spongiform encephalopathy. Definitive diagnosis of TSE in livestock is currently based on a combination of postmortem testing including histopathology, immunohistochemistry, and molecular techniques, but electroretinography may provide a new TSE screening strategy for live cattle.

Materials and Methods

Animals

Five 9 month old Holstein steers were inoculated intracerebrally with brain homogenate prepared from a second-passage TME-affected steer from a prior experiment[4]. Antemortem testing (electroretinography, see below) was performed at monthly intervals prior to the onset of clinical signs of disease for all cattle, and 1 or 2.5 weeks prior to euthanasia for 2/5 cattle. All cattle developed clinical disease characterized by loss of body condition, locomotor abnormalities, frequent falls, and difficulty rising, and were euthanized when deemed humanely necessary (3/5 at 16.8 (2 steers) and 16.9 months post-inoculation (PI), and 2/5 at 19.3 and 19.6 mo. PI). Eyes from 3 non-inoculated Holstein cattle were used as controls for histology and immunohistochemistry. Ten approximately age-matched, non-inoculated, Holstein steers housed in the same building as the TME-inoculated cattle served as the control cohort for ERG analysis. All animal procedures had the approval of the National Animal Disease Center's Animal Care and Use Committee.

Electroretinography

Holstein steers were used to gather normative (n=10) and TSE-associated (n=5) ERG data. ERG data was collected from TME-inoculated steers prior to clinical signs of disease at 12.5, 13.5, and 14.5 months post-inoculation (5/5), and at 18.5 mo. PI (1-3 weeks prior to euthanasia due to clinical disease) (2/5). Animals were lightly sedated with 0.02 mg/kg xylazine prior to auriculopalpebral nerve block with 2% lidocaine and electrode placement. Pupillary dilation was induced with topical administration of 1% tropicamide ophthalmic solution to the cornea. One eye was tested in each animal.

A DTL Plus microfiber electrode (LKC Technologies, Gaithersburg, MD) was placed on the unanesthetized cornea, and subdermal 12 mm, 29 gauge needle electrodes (LKC Technologies, Gaithersburg, MD) were used as reference and ground. The reference electrode was placed subcutaneously approximately 2 cm caudal to the lateral canthus, and the ground electrode was placed subcutaneously in the region overlying the occipital bone. An EPIC 4000 visual electrodiagnostic testing system (LKC Technologies, Gaithersburg, MD) with a CMGS-1 Color Mini-Ganzfeld Stimulator (LKC Technologies, Gaithersburg, MD) was used to conduct the ERG experiments. Cattle were dark adapted for 20 minutes,

followed by a series of 2 scotopic recordings, 10 minutes of light adaptation, and 1 photopic recording.

The b-wave amplitude and implicit time was measured for each ERG. The non-inoculated group was compared to the preclinical TME-inoculated group using the Mann-Whitney *U* test with a 95% confidence interval. *P* values less than 0.05 were regarded as statistically significant.

Histopathology

Entire globes with a segment of optic nerve were extracted at necropsy, and immersed in Bouin's fixative for at least 24 hours followed by immersion in alkaline alcohol. A 5 mm thick vertical section from the caudal aspect of the globe containing retina and optic nerve were processed by routine histological methods and embedded into paraffin blocks. Serial 4 μm sections were cut from the retina and stained with hematoxylin and eosin.

Immunohistochemistry

The distribution of PrP^{Sc} and various retinal cell type-specific markers in the retinas of 3 control and 5 TME-affected cattle were examined. Slides were immunolabeled to detect PrP^{Sc} as previously described[8] using primary antisera containing monoclonal antibodies F89/160.5[25] and F99/97.6.1[26] each at a concentration of 5 μM/ml. Sections immunolabeled to detect retinal cell type-specific antigens were processed as previously described.[14] Labeling patterns were imaged with a fluorescence-capable microscope (Nikon Eclipse E800) equipped with a digital camera, and prepared using Adobe Photoshop CS Version 8.0 and Macromedia Freehand MX Version 11.0 for the Macintosh.

Primary antibodies used in this study included the following: rabbit anti-protein kinase C-alpha isoform (PKCα) (Sigma, St. Louis, MO); guinea pig anti-vesicular glutamate transporter 1 (VGLUT1) (Chemicon International, Inc., Temecula, CA); rabbit anti-glutamine synthetase (GS) (Sigma, St. Louis, MO); and rabbit anti-glial fibrillary acidic protein (GFAP) (DakoCytomation, Carpinteria, CA). Secondary antibodies included fluorescein isothiocyanate (FITC)-conjugated donkey anti-guinea pig IgG (Jackson ImmunoResearch, West Grove, PA); or FITC-conjugated donkey anti-rabbit IgG (Jackson ImmunoResearch, West Grove, PA).

Acknowledgments

We thank Leisa Mandell, M. Church, and J. Lesan for technical assistance. This work was supported by Specific Cooperative Agreement #58-3625-5-114 with the Agricultural Research Service, USDA. Mention of trade names or commercial products in this paper is solely for the purpose of providing specific information and does not imply recommendation or endorsement by the U.S. Department of Agriculture.

References

1. Collinge, J., Sidle, K. C., Meads, J., Ironside, J. & Hill, A. F. Molecular analysis of prion strain variation and the aetiology of 'new variant' CJD. Nature 383, 685-90 (1996).
2. Bruce, M. E. et al. Transmissions to mice indicate that 'new variant' CJD is caused by the BSE agent. Nature 389, 498-501 (1997).
3. Robinson, M. M. et al. Experimental infection of cattle with the agents of transmissible mink encephalopathy and scrapie. J Comp Pathol 113, 241-51 (1995).
4. Hamir, A. N., Kunkle, R. A., Miller, J. M., Bartz, J. C. & Richt, J. A. First and second cattle passage of transmissible mink encephalopathy by intracerebral inoculation. Vet Pathol 43, 118-26 (2006).
5. Bradley, R. BSE transmission studies with particular reference to blood. Dev Biol Stand 99, 35-40 (1999).
6. Foster, J., Farquhar, C., Fraser, J. & Somerville, R. Immunolocalization of the prion protein in scrapie affected rodent retinas. Neurosci Lett 260, 1-4 (1999).
7. Greenlee, J. J., Hamir, A. N. & West Greenlee, M. H. Abnormal prion accumulation associated with retinal pathology in experimentally inoculated scrapie-affected sheep. Vet Pathol 43, 733-9 (2006).
8. Hamir, A. N. et al. Transmission of sheep scrapie to elk (Cervus elaphus nelsoni) by intracerebral inoculation: final outcome of the experiment. J Vet Diagn Invest 16, 316-21 (2004).
9. Head, M. W. et al. Prion protein accumulation in eyes of patients with sporadic and variant Creutzfeldt-Jakob disease. Invest Ophthalmol Vis Sci 44, 342-6 (2003).
10. Hortells, P. et al. Pathological findings in retina and visual pathways associated to natural Scrapie in sheep. Brain Res 1108, 188-94 (2006).
11. Jeffrey, M. et al. Onset and distribution of tissue PrP accumulation in scrapie-affected suffolk sheep as demonstrated by sequential necropsies and tonsillar biopsies. J Comp Pathol 125, 48-57 (2001).
12. Spraker, T. R. et al. Comparison of histological lesions and immunohistochemical staining of proteinase-resistant prion protein in a naturally occurring spongiform encephalopathy of free-ranging mule deer (*Odocoileus hemionus*) with those of chronic wasting disease of captive mule deer. Vet Pathol 39, 110-9 (2002).
13. Valdez, R. A., Rock, M. J., Anderson, A. K. & O'Rourke, K. I. Immunohistochemical detection and distribution of prion protein in a goat with natural scrapie. J Vet Diagn Invest 15, 157-62 (2003).

14. Smith, J. D., Greenlee, J. J., Hamir, A. N. & West Greenlee, M. H. Retinal cell types are differentially affected in sheep with scrapie. J Comp Pathol 138, 12-22 (2008).
15. Curtis, R., Fraser, H., Foster, J. D. & Scott, J. R. The correlation of electroretinographic and histopathological findings in the eyes of mice infected with the 79A strain of scrapie. Neuropathol Appl Neurobiol 15, 75-89 (1989).
16. de Seze, J. et al. Creutzfeldt-Jakob disease: neurophysiologic visual impairments. Neurology 51, 962-7 (1998).
17. Katz, B. J., Warner, J. E., Digre, K. B. & Creel, D. J. Selective loss of the electroretinogram B-wave in a patient with Creutzfeldt-Jakob disease. J Neuroophthalmol 20, 116-8 (2000).
18. Frishman, L. Origins of the electroretinogram. In Heckenlively JR and Arden GB (eds): Priniciples and practice of clinical electrophysiology of vision, 2nd Ed. Cambride, MA, MIT Press. (ed. Heckenlively JR, A. G.) (MIT Press, Cambridge, MA, 2006).
19. Haverkamp, S. & Wassle, H. Immunocytochemical analysis of the mouse retina. J Comp Neurol 424, 1-23 (2000).
20. Johnson, J. et al. Vesicular neurotransmitter transporter expression in developing postnatal rodent retina: GABA and glycine precede glutamate. J Neurosci 23, 518-29 (2003).
21. Wong, B. S. et al. Oxidative impairment in scrapie-infected mice is associated with brain metals perturbations and altered antioxidant activities. J Neurochem 79, 689-98 (2001).
22. Wong, B. S. et al. Increased levels of oxidative stress markers detected in the brains of mice devoid of prion protein. J Neurochem 76, 565-72 (2001).
23. Chiarini, L. B. et al. Cellular prion protein transduces neuroprotective signals. Embo J 21, 3317-26 (2002).
24. Armstrong, R. A. Creutzfeldt-Jakob disease and vision. Clin Exp Optom 89, 3-9 (2006).
25. O'Rourke, K. I. et al. Monoclonal antibody F89/160.1.5 defines a conserved epitope on the ruminant prion protein. J Clin Microbiol 36, 1750-5 (1998).
26. Spraker, T. R. et al. Validation of monoclonal antibody F99/97.6.1 for immunohistochemical staining of brain and tonsil in mule deer (*Odocoileus hemionus*) with chronic wasting disease. J Vet Diagn Invest 14, 3-7 (2002).

Figure Legends

Figure 1. Representative electroretinograms (ERGs) from non-inoculated control (**a, c, e**) and preclinical (14.5 months PI) TME-inoculated Holstein cattle (**b, d, f**). ERGs elicited with photostimuli of two varying intensities under scotopic (dark-adapted) testing conditions are shown (**a-d**). The b-wave is the large positive deflection. Photopic (light-adapted) ERG responses are also shown (**e,f**).

Figure 2. Electroretinogram b-wave data from non-inoculated and preclinical TME-inoculated cattle. (**a**) Comparison of b-wave implicit time data among control and preclinical TME cattle at serial post-inoculation (PI) time points under scotopic testing conditions using a low intensity light stimulus. Implicit time was significantly prolonged in TME-inoculated cattle versus controls at all time points. (**b**) The experiment was carried out as described in **a**, but ERGs were elicited with a higher intensity light stimulus. A statistically significant difference was observed between controls and the TME group at 13.5 and 14.5 months PI. (**c**) Cattle were light-adapted and ERGs were elicited with the same stimulus intensity as in **b**. Implicit times were significantly prolonged in the TME-inoculated group versus controls. (**d**) Mean b-wave amplitude and implicit time values (± SD) for control (n=10), preclinical (n=5), and clinical (n=2) TME-inoculated cattle. Implicit time data included here is that represented in **a-c**. Significant differences in b-wave amplitude among controls and preclinical TME-inoculated cattle were not detected. Abbreviations: cd•s/m^2, candela seconds per meter squared; PI, post-inoculation. ***P<0.001, **P<0.01, *P<0.05 versus control group.

Figure 3. Retinal histology and distribution of abnormal prion protein (PrP^{Sc}) in the retinas of control (**a, c**) and TME-affected (**b, d**) cattle. Retinal sections from control (**a**) and TME-affected (**b**) cattle stained with hematoxylin and eosin revealed subtle changes in TME-affected retinas, such as multifocal, distinct, clear spaces within the IPL (arrows) and decreased numbers of nuclei in the GCL. PrP^{Sc} was not detected in control retina (**c**), but intense punctate PrP^{Sc}-immunoreactivity was detected throughout both plexiform layers, within retinal ganglion cells (arrow), and sporadically within the inner nuclear layer and at the outer limiting membrane (arrowheads) in retinas from TME-affected cattle (**d**). Abbreviations: OS, outer segments; ONL, outer nuclear layer; OPL, outer plexiform layer; INL, inner nuclear layer; IPL, inner plexiform layer; GCL, ganglion cell layer. Scale bars = 20μm.

Figure 4. Immunoreactivity (-IR) patterns of PKCα, VGLUT1, GS, and GFAP in the retinas of control (**a-d**) and TME-affected (**e-h**) cattle. Compared to control retinas (**a**), PKCα-IR in

TME-affected retinas (**e**) was less uniform across the OPL, and rod bipolar cell terminals were less obvious as larger, ovoid puncta of –IR. VGLUT1-immunoreactive bipolar cell terminals (arrows **b,f**) in TME-affected retinas were less prominent along the vitreal border of the IPL compared to control retinas. Relative to control retinas (**c**), GS-IR in TME-affected retinas (**g**) was increased in Müller glial processes coursing through the IPL. GFAP-positive radial processes were more numerous and prominent in TME-affected cattle (**h**) versus controls (**d**). Abbreviations: OS, outer segments; ONL, outer nuclear layer; OPL, outer plexiform layer; INL, inner nuclear layer; IPL, inner plexiform layer; GCL, ganglion cell layer; OFL, optic fiber layer. Scale bars = 20μm.

Figure 1.

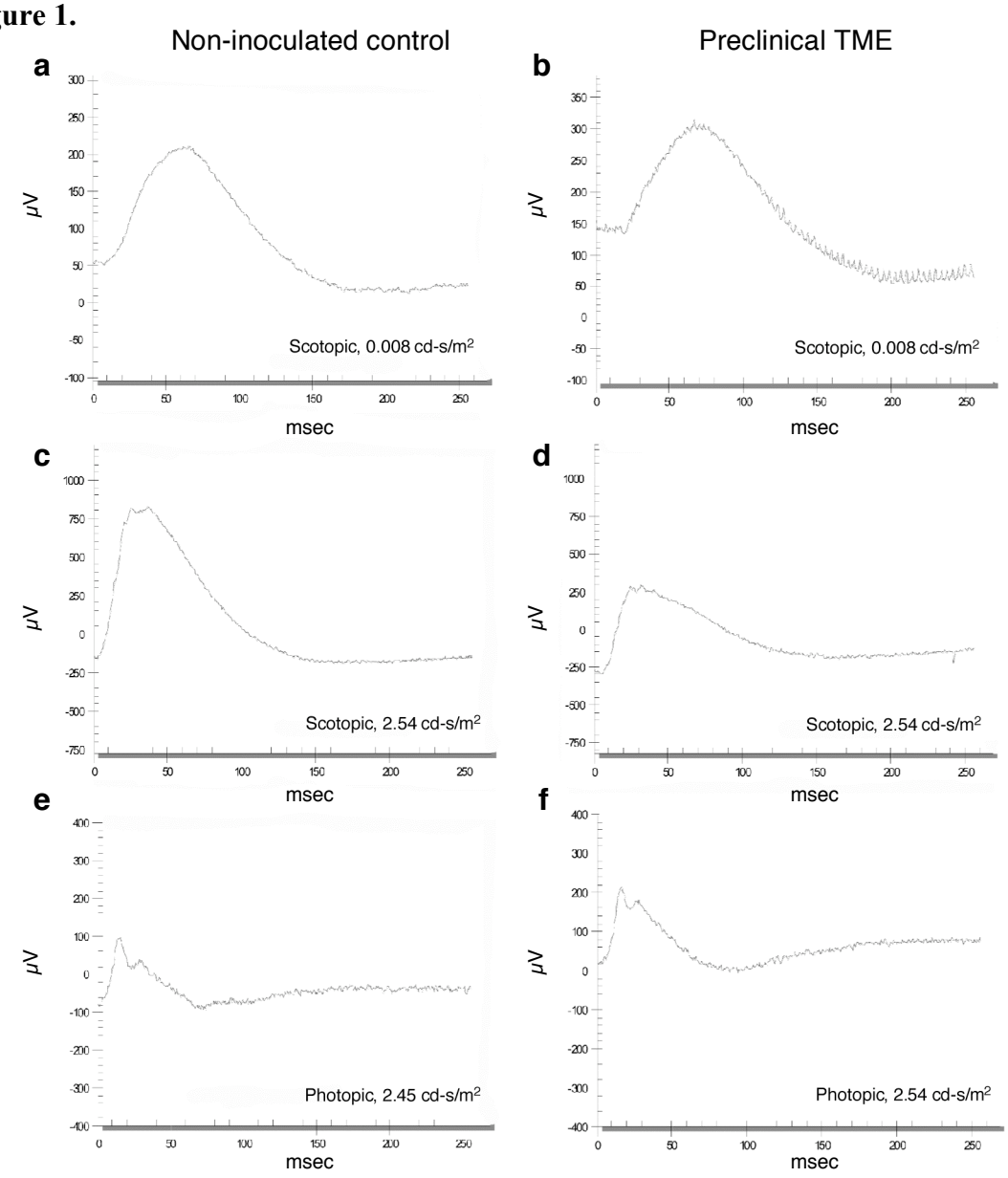
Non-inoculated control
Preclinical TME
a
b
c
d
e
f
μV
msec
Scotopic, 0.008 cd-s/m2
Scotopic, 2.54 cd-s/m2
Photopic, 2.45 cd-s/m2
Photopic, 2.54 cd-s/m2

Figure 2.

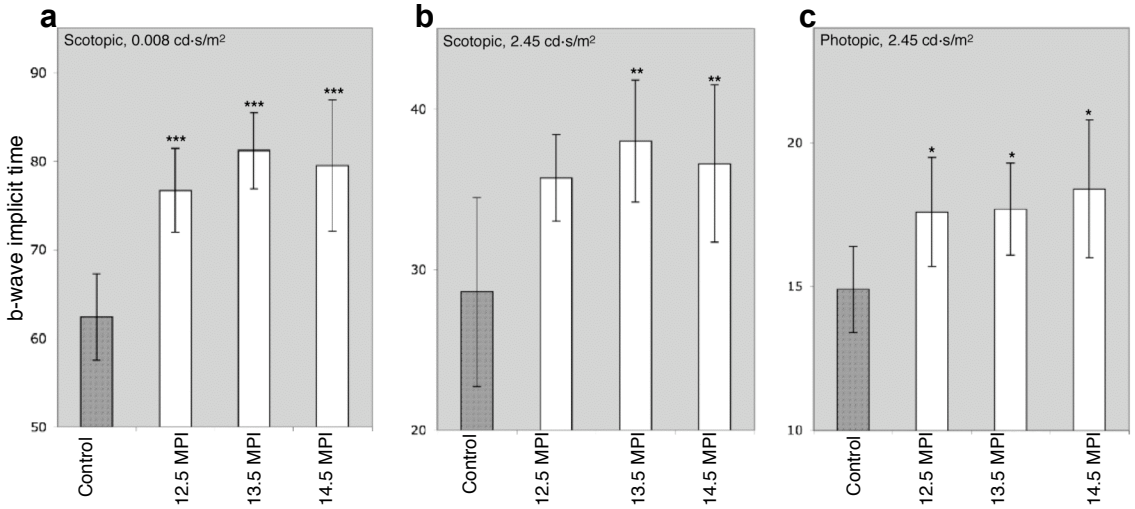

d

Test	Test Condition	Experimental Condition	Mean b-wave amplitude (μV) ± SD	Mean b-wave implicit time (msec) ± SD
1	Scotopic, -0.008 cd•s/m^2	TME – 12.5 mo. PI	149.2 ± 65.5	77.0 ± 4.7***
		TME – 13.5 mo. PI	159.9 ± 31.6	81.2 ± 4.3***
		TME – 14.5 mo. PI	174.6 ± 48.3	79.5 ± 7.4***
		TME – 18.5 mo. PI[#]	77.3 ± 15.8	73.1 ± 5.3
		Non-inoculated	140.3 ± 51.5	62.4 ± 4.9
2	Scotopic, 2.45 cd•s/m^2	TME – 12.5 mo. PI	558.1 ± 168.0	35.7 ± 5.9
		TME – 13.5 mo. PI	549.5 ± 160.0	38.0 ± 2.7**
		TME – 14.5 mo. PI	552.3 ± 151.4	36.6 ± 3.8**
		TME – 18.5 mo. PI[#]	164.4 ± 36.0	36.2 ± 18.2
		Non-inoculated	720.6 ± 227.1	28.6 ± 4.9
3	Photopic, 2.45 cd•s/m^2	TME – 12.5 mo. PI	121.3 ± 41.8	17.6 ± 1.9*
		TME – 13.5 mo. PI	116.5 ± 26.6	17.7 ± 1.6*
		TME – 14.5 mo. PI	105.4 ± 54.1	18.4 ± 2.4*
		TME – 18.5 mo. PI[#]	66.3 ± 13.4	14.7 ± 0.2
		Non-inoculated	152.1 ± 55.5	14.9 ± 1.5

***p<0.001, **p<0.01, *p<0.05; Mann-Whitney *U* test
[#] Data from two animals; statistical analyses not performed.

Figure 3.

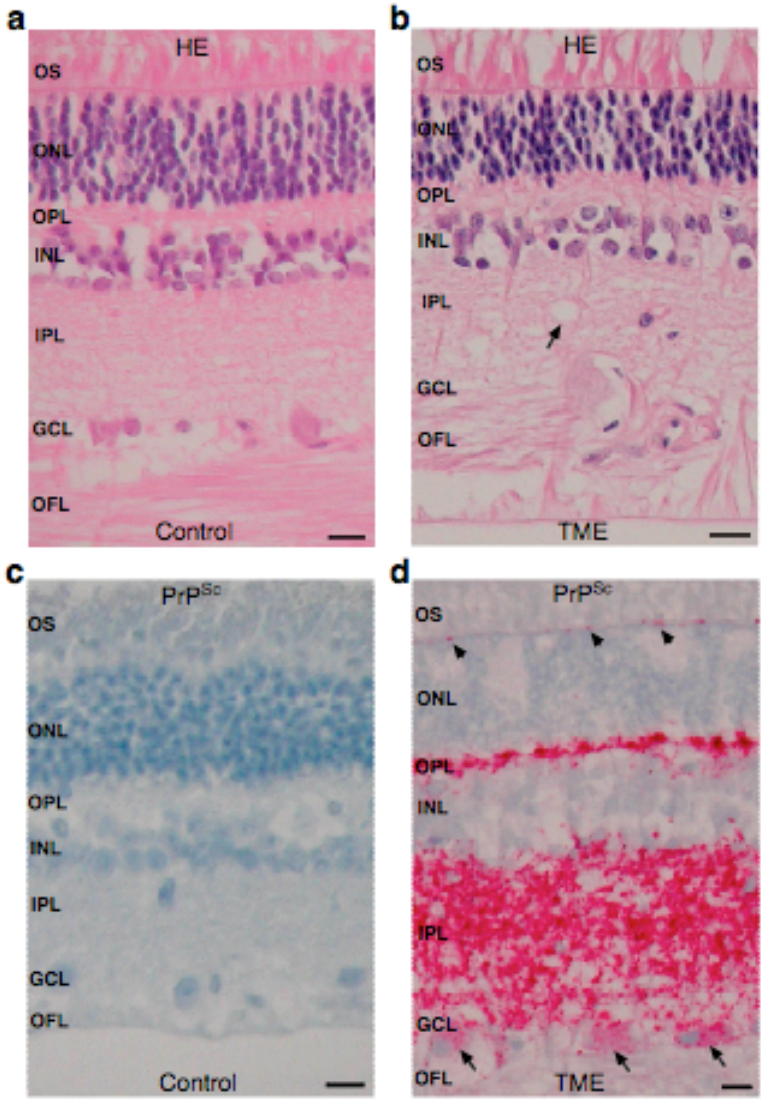
a
HE
OS
ONL
OPL
INL
IPL
GCL
OFL
Control
b
HE
OS
ONL
OPL
INL
IPL
GCL
OFL
TME
c
PrPSc
OS
ONL
OPL
INL
IPL
GCL
OFL
Control
d
PrPSc
OS
ONL
OPL
INL
IPL
GCL
OFL
TME

Figure 4.

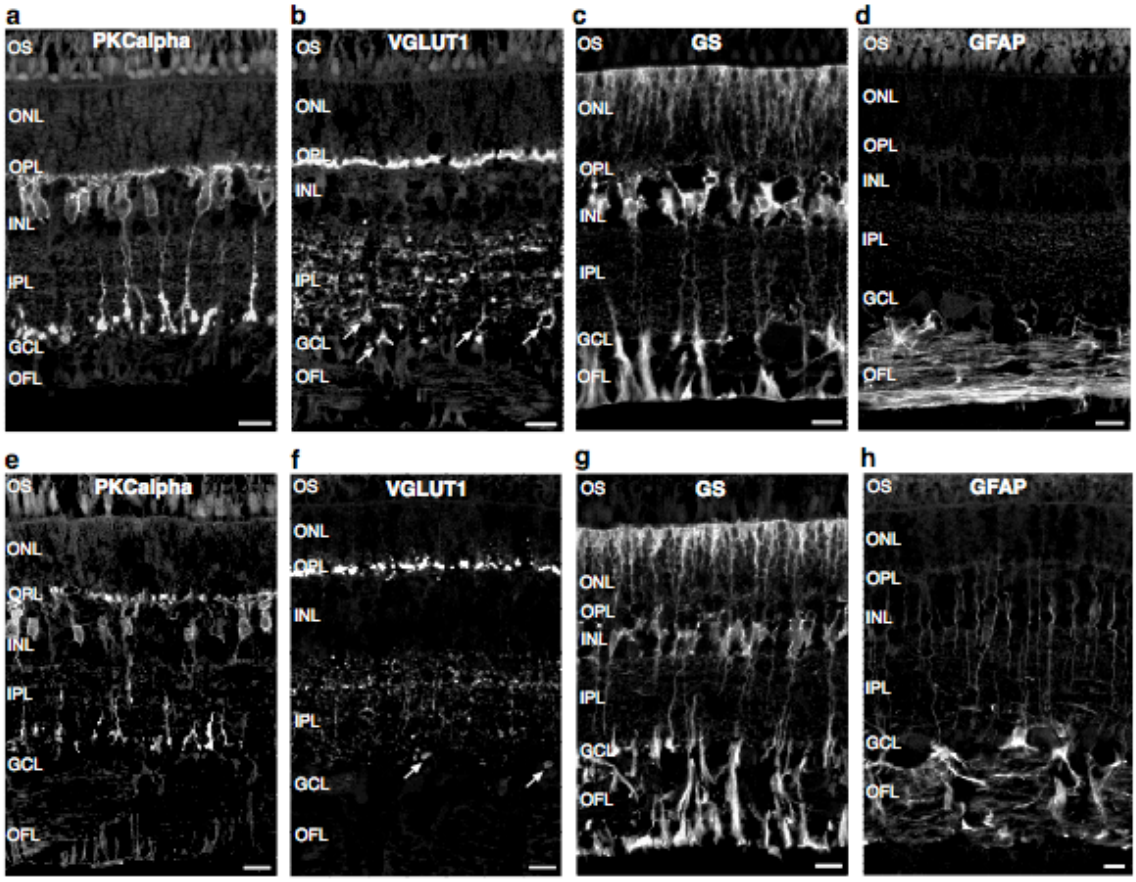
a
PKCalpha
b
VGLUT1
c
GS
d
GFAP
e
PKCalpha
f
VGLUT1
g
GS
h
GFAP
OS
ONL
OPL
INL
IPL
GCL
OFL

CHAPTER 4. GENERAL CONCLUSIONS

Summary

The transmissible spongiform encephalopathies, with their unique and somewhat controversial causal agent and incompletely understood pathogenesis, present an intriguing research problem. The specific effects abnormal prion protein (PrP^{Sc}) may have on cells of the nervous system is largely unknown, therefore, the goal of this dissertation was to examine these potential effects on cellular morphology and function within the neural retina. This dissertation addressed the effects of PrP^{Sc} accumulation on retinal morphology in sheep infected with scrapie. It also examined the effects of PrP^{Sc} on both retinal morphology and function in cattle infected with transmissible mink encephalopathy (TME). We have demonstrated that accumulation of PrP^{Sc} in the retinas of scrapie affected sheep results in altered morphology of some retinal cell types, but not all. We have also shown that PrP^{Sc} accumulation in the retinas of cattle infected with TME results in disruption of both retinal function and morphology. Determining the effects of PrP^{Sc} on specific retinal cell types will be important for advancing understanding of the pathogenesis of these neurodegenerative diseases. Our findings contribute novel and important information on the response of the retina to TSE.

In chapter two, the effects of PrP^{Sc} accumulation on the retinas of sheep clinically affected with scrapie were investigated. PrP^{Sc} has been shown to accumulate in the retinas of sheep with scrapie without overt evidence of retinal degeneration.[1, 2] Whether PrP^{Sc} accumulation is actually adversely affecting retinal cells is an important question to address. By examining retinal sections using various cell type specific antibodies, we demonstrated altered immunoreactivity patterns of rod bipolar, retinal ganglion, and Müller glia cell markers in the retinas of scrapie-affected sheep. Immunoreactivity patterns of cholinergic amacrine cells and conventional synapses were similar to controls. From these observations, we concluded that retinal cell types are differentially affected by PrP^{Sc} accumulation in scrapie-affected sheep. These results lend support to the hypothesis that retinal cellular morphology is affected in TSE-infected livestock species, and provide insight into what cell types may be preferentially affected by PrP^{Sc} accumulation in the nervous system.

In chapter three, we examined the effects of PrP^{Sc} accumulation on the retinas of cattle infected with TME prior to the onset of clinical disease (functional analysis) and during the clinical course of disease (functional and morphologic analyses). To date, there is an absence of information regarding specific functional and morphologic alterations in the retinas of TSE-infected cattle. We evaluated retinal function in Holstein steers, intracerebrally inoculated with TME, using electroretinography. We demonstrated prolonged ERG b-wave implicit time during preclinical stages of disease, and both prolonged implicit time and decreased amplitude of the ERG b-wave in clinically affected cattle. Both scotopic and photopic responses were affected. Histologic assessment of hematoxylin and eosin stained retinal sections revealed evidence of spongiform change in the IPL and decreased cell density in the GCL in TME-affected cattle. Using immunohistochemistry, we were also able to demonstrate marked PrP^{Sc} accumulation and altered rod bipolar cell and Müller glia morphology in the retinas of TME-affected cattle. These results also support the central hypothesis of this doctoral work, and contribute initial information on the functional and morphologic consequences of TSE on the bovine retina.

Recommendations for Future Research

Cellular localization of PrP^{Sc} in the retina

We have shown that PrP^{Sc} is present in the retinas of TSE-affected sheep and cattle, and that immunoreactivity patterns of specific retinal cell types are altered in these animals. What remains unknown is the specific subcellular localization of PrP^{Sc} within the retina. Subcellular localization of PrP^{Sc} within the retina could be investigated through double-label immunohistochemistry using PrP specific and various retinal cell type specific markers, followed by confocal microscopic analysis to assess for colocalization of signals. This would also allow for three-dimensional reconstruction, which may aid in determining a more precise localization pattern. Colocalization studies have been successfully performed on the brain of humans with CJD.[3] Additionally, retinal sections could be prepared for immunoelectron microscopy using antibodies directed against PrP. However, there is currently not an antibody available that specifically recognizes PrP^{Sc} (over PrP^{C}), and common pretreatments used to degrade PrP^{C} (so only proteinase-resistant PrP^{Sc} remains for detection) inevitably destroy cellular ultrastructure. PrP^{Sc} in the retinas of TSE-affected

animals is most likely more abundant than PrP^{C}, so the majority of labeled protein could be surmised to be PrP^{Sc}, but this would carry the caveat that a certain proportion is likely residual native PrP^{C}.

Investigation of synaptic protein profiles in the retinas of TSE affected animals

We, and others, have shown that PrP^{Sc} accumulates primarily within the synaptic layers of the retina of TSE-affected animals. A number of studies have also shown that the normal cellular isoform of the prion protein, PrP^{C}, is localized to synaptic structures in the CNS. Our electroretinography results demonstrate that retinal function is altered in TSE-infected cattle, and we hypothesize that disruption of synaptic proteins could be one contributing factor. Altered synaptic protein expression has been demonstrated in the brain of scrapie-infected mice[4] and in the cerebellum of humans affected with CJD.[5] Synaptic protein profiles in the retinas of TSE-infected sheep and cattle (and other species) could be investigated using immunohistochemistry to compare the distribution of various synapse related proteins (e.g. core SNARE complex proteins, synaptophysin) between TSE-infected animals and controls. Additionally, Western blot analysis of retinas using antibodies directed against synaptic proteins could provide a semi-quantitative method of determining differences in synaptic protein profiles between infected and control animals.

Evaluation of retinal function and morphology in cattle infected with bovine spongiform encephalopathy

The studies conducted on cattle in this dissertation examined the effects of the TSE transmissible mink encephalopathy on retinal cellular morphology and function. While the histopathologic picture of TME in cattle is similar to that of BSE in cattle, cattle are not the natural hosts of TME. Studying this TSE in cattle is an initial step in examining the effects of PrP^{Sc} on the bovine retina, but the retina should also be studied in cattle infected with BSE, their naturally occurring TSE. The effects of PrP^{Sc} accumulation in natural versus non-natural host species can differ substantially. For example, scrapie-affected sheep (natural host) with demonstrable retinal PrP^{Sc} accumulation do not appear to have associated major morphologic changes in their retinas.[2] Retinas from scrapie-affected hamsters and mice, however, exhibit extensive photoreceptor degeneration.[6-8] Morphologic studies similar to those reported in this dissertation could be performed to investigate the effects of PrP^{Sc}

accumulation on retinal cellular morphology in BSE-infected cattle. Additionally, retinal ganglion cell numbers could be compared between control and BSE-infected cattle by quantifying axons in cross sections of optic nerve. We reported a decrease in the number of cells within the ganglion cell layer in TME-affected cattle versus controls. The expression levels of various cell type specific proteins, especially those identified by immunohistochemistry, could be compared with Western blot analysis. This would provide a semi-quantitative analysis of the expression level of chosen retinal cell type specific markers.

Concluding Remarks

This doctoral work has addressed some of the effects of PrP^{Sc} accumulation on retinal cellular morphology and function. By demonstrating that specific retinal cellular morphologies are affected by PrP^{Sc} accumulation, we have provided additional insight into the specific effects of PrP^{Sc} on cells of the nervous system. This work also provides the first direct evidence of altered retinal function in a non-rodent TSE-infected host, providing information on the functional consequences of retinal PrP^{Sc} accumulation in a natural host of a TSE. Additionally, these findings provide support for the concept of utilizing electroretinography as a screening tool for TSE in cattle.

References

1. Jeffrey, M. et al. Onset and distribution of tissue PrP accumulation in scrapie-affected suffolk sheep as demonstrated by sequential necropsies and tonsillar biopsies. J Comp Pathol 125, 48-57 (2001).
2. Greenlee, J. J., Hamir, A. N. & West Greenlee, M. H. Abnormal prion accumulation associated with retinal pathology in experimentally inoculated scrapie-affected sheep. Vet Pathol 43, 733-9 (2006).
3. Kovacs, G. G., Preusser, M., Strohschneider, M. & Budka, H. Subcellular localization of disease-associated prion protein in the human brain. Am J Pathol 166, 287-94 (2005).
4. Siso, S. et al. Abnormal synaptic protein expression and cell death in murine scrapie. Acta Neuropathol (Berl) 103, 615-26 (2002).
5. Ferrer, I., Puig, B., Blanco, R. & Marti, E. Prion protein deposition and abnormal synaptic protein expression in the cerebellum in Creutzfeldt-Jakob disease. Neuroscience 97, 715-26 (2000).
6. Buyukmihci, N., Rorvik, M. & Marsh, R. F. Replication of the scrapie agent in ocular neural tissues. Proc Natl Acad Sci U S A 77, 1169-71 (1980).
7. Buyukmihci, N., Goehring-Harmon, F. & Marsh, R. F. Photoreceptor degeneration preceding clinical scrapie encephalopathy in hamsters. J Comp Neurol 205, 49-54 (1982).

8. Hogan, R. N., Baringer, J. R. & Prusiner, S. B. Progressive retinal degeneration in scrapie-infected hamsters: a light and electron microscopic analysis. Lab Invest 44, 34-42 (1981).